University of Zurich[UZH]

Tree-ring based reconstruction of past snow avalanches using two tree species at a slope in the Göscheneralp

GEO 511 Master's Thesis

Author
Philipp Rüegg
16-707-598

Supervised by
Prof. Dr. Paolo Cherubini (paolo.cherubini@wsl.ch)
Dr. Holger Gärtner (holger.gaertner@wsl.ch)

Faculty representative
Prof. Dr. Markus Egli

31.01.2022
Department of Geography, University of Zurich

Master's Thesis - University of Zurich

Tree-ring based reconstruction of past snow avalanches using two tree species at a slope in the Göscheneralp

Author:
Philipp Rüegg

Supervised by:
Prof. Dr. Paolo Cherubini, WSL
Dr. Holger Gärtner, WSL

Faculty representative:
Prof. Dr. Markus Egli, University of Zurich

Acknowledgments

Foremost, I would like to thank Prof. Dr. Paolo Cherubini for his initial research idea, his enthusiastic mediation of dendrochronology and quick support whenever needed. Likewise, Dr. Holger Gärtner for his continuing guidance and expertise during the whole thesis.

Loïc Schneider is to be thanked for his assistance in the lab and for providing storage room for my samples. In addition, Anne Verstege, who provided valuable input for cross-dating and measuring tree-ring widths. Special thanks go to Nadja-Tamara Studer for her indispensable aid during sampling and invaluable assistance during many hours of lab work. Also, to Ferdi Herger, for providing the permission to take samples at the Göscheneralp. Further, I would like to thank Niklaus Brunner for proofreading my thesis. Moreover, my gratitude goes to Lisa Maria Pirisinu for providing emotional support and to Silja Eller for fun hours during sampling trips. At last, I would like to thank the other master students for providing good company and motivation during coffee breaks, namely Nicola Paltenghi, Davide Bernasconi, Ariane Dieth, Kurt Weber and Annatina Hassler.

Abstract

Snow avalanches pose a major threat to people living in mountainous regions across the world. Chronologies of such events date back centuries and are often focused on larger events and substantial damage to people and infrastructure. Dendrochronology offers methods to reconstruct snow avalanches at a specific site, when no records are available. In this thesis, silver birch (*Betula Pendula* Roth) and mountain pine (*Pinus mugo* Turra) were used in order to reconstruct snow avalanches at a site at the Göscheneralp, Uri. For this purpose, increment cores and discs were extracted and thin sections produced. Event dating was done by means of an eccentricity analysis as well as compression wood findings. Furthermore, the findings were compared to an existing snow avalanche chronology. As a result, snow avalanches were determined to have happened in years 1999, 2008, 2010, 2012, 2019 and 2021. In addition, snow avalanches were also spatially defined. The findings serve as a reasonable approximation, however should not be taken unambiguously.

Contents

List of Figures

List of Tables

1 Introduction

Snow avalanches have affected people in mountainous regions ever since settlements were built and remains one of the most active hazards in these regions. Especially in the alps, where the first settlements date back hundreds to thousands of years, high damage tolls have been experienced over the years. For this reason, protection forests have been established. One example can be found just above Andermatt, Uri, where even the removal of cones or branches is banned since 1397. Nowadays, it still serves as a protective forest, also called "Bannwald", sheltering against snow avalanches and rockfalls (Brang et al., 2008; Renner-Aschwanden, 2013).

Snow avalanches occur on distinct sites, promoted not only by the meteorological conditions, but also topographical situation and the amount of forest cover. If a snow avalanche happens repeatedly at a site, forest growth is halted and an open area or corridor is established, also called a snow avalanche slope. In many cases, the vegetation growing in and along these slopes changes from mature forest to more shrub-like and low growing trees (Butler et al., 2008; Luckman, 2010).

The earliest chronologies of snow avalanches can be dated back to the 14th century and provide an essential source of information to infer hazard zones in and around settlements. Next to actual listings of snow avalanches, the analysis of earlier photographs, eyewitnesses reports, as well as vegetation studies can be consulted (Corona et al., 2012). As an example, Butler et al. (1985) used historic coverings of snow avalanches, such as personal recollections, photographs, text citations and newspaper coverage in combination with tree-ring data to reconstruct snow avalanches in Montana. A big shortcoming of historic snow avalanche chronologies is the limited temporal and spatial information. Mainly, the documented events focus on damage to roads and settlements as well as harm to population. Besides, eyewitness reports tend to have a bias in their focus, exaggerating some events and downplaying others (Bollschweiler et al., 2011; Corona et al., 2012). For that reason, dendrochronology and dendrogeomorphology offer an excellent chance to get an overview of the events happening at a specific site and possibly also providing hazard assessments (Corona et al., 2012). Studies to reconstruct snow avalanches through dendrochronological methods have been done as early as the 1970s by Burrows et al. (1976) which give an overview over using tree rings to date snow avalanches, as well as (Carrara, 1979), producing a record of when snow avalanches reached a settlement in Colorado. More recent studies have been done by Casteller et al. (2007), using multiple dendroecological methods to uncover a snow avalanche history. Similar methods have also been used in other studies (Butler et al., 2008; Decaulne et al., 2011; Dube et al., 2004; Germain et al., 2010).

Eccentricity, often used in the reconstruction of geomorphic mass movements (Wistuba et al., 2013), has of late also been used to date snow avalanches (Casteller et al., 2008; Casteller et al., 2007, 2011; Decaulne et al., 2011; Garavaglia et al., 2011). Eccentricity in combination with reaction wood, disturbances and deformations of wood has so far not been widely studied (Schweingruber, 1996). This work will focus on combining reaction wood and eccentricity in trees. No focus will be given on the nature and physics of snow avalanches, as has been done in simulations (Casteller et al., 2008). The aim of this thesis is to reconstruct past snow avalanches. This will be done by constructing and

using an eccentricity index of a deciduous species as well as comparing it to an existing chronology. This will then also be compared to reaction wood in conifers, in order to possibly verify past snow avalanche events. The relevance behind this thesis is, to use two very rarely used tree species and to successfully show that snow avalanche reconstructions are possible with these. In addition, snow avalanche frequencies serves as an important planning tool for land-use planning and management (Corona et al., 2010).

1.1 Research objectives

The goal of this master thesis is to acquire a snow avalanche reconstruction using silver birch (*Betula Pendula* Roth) and mountain pine (*Pinus mugo* Turra) in the Göscheneralp, Uri, by working out past events. An eccentricity index of the birch will be constructed and then compared to compression wood in mountain pine. The first [1] objective is to see, if it is possible in the first place, to make a snow avalanche reconstruction by also comparing to known chronologies. Also referring to Corona et al. (2012), of how much of the actual snow avalanche activity can be proven with dendrogeomorphic methods. The second [2] objective is to compare eccentricity thresholds and their influence on the dating of snow avalanche events. Another objective [3] is to set eccentricity index events side by side to compression wood in pine, and therefore show if an snow avalanche event can be verified in both species during the same year or period. The first subquestion revolves around if the tension wood in birch can be determined anatomically, whereas the second subquestion aims to date snow avalanche events also with injuries in the birch samples. Eventually, the last research objective [4] asks, if the dated snow avalanches do differ in their spatial extent at the study site. Consecutively a listing of the research questions:

1. Do the dated snow avalanche events coincide with an already existing chronology?
2. Can an accurate eccentricity threshold be chosen?
   (a) How to the determined events differ, if the threshold is altered?
3. Can the dated eccentricity in birch be compared to compression wood formation in pine?
   (a) Is it possible to anatomically determine tension wood in birch and therefore verify dated eccentricity events?
   (b) Is it possible to compare injuries in birch trees to dated eccentricity events?
4. Can the dated snow avalanche reconstruction be spatially defined?

2 Study site

The study site is located in the Göscheneralp (46°38'N 8°54'E) and is easy accessible at a five minute drive from Göschenen (see figure 1). What follows is a brief description of key features of the location.

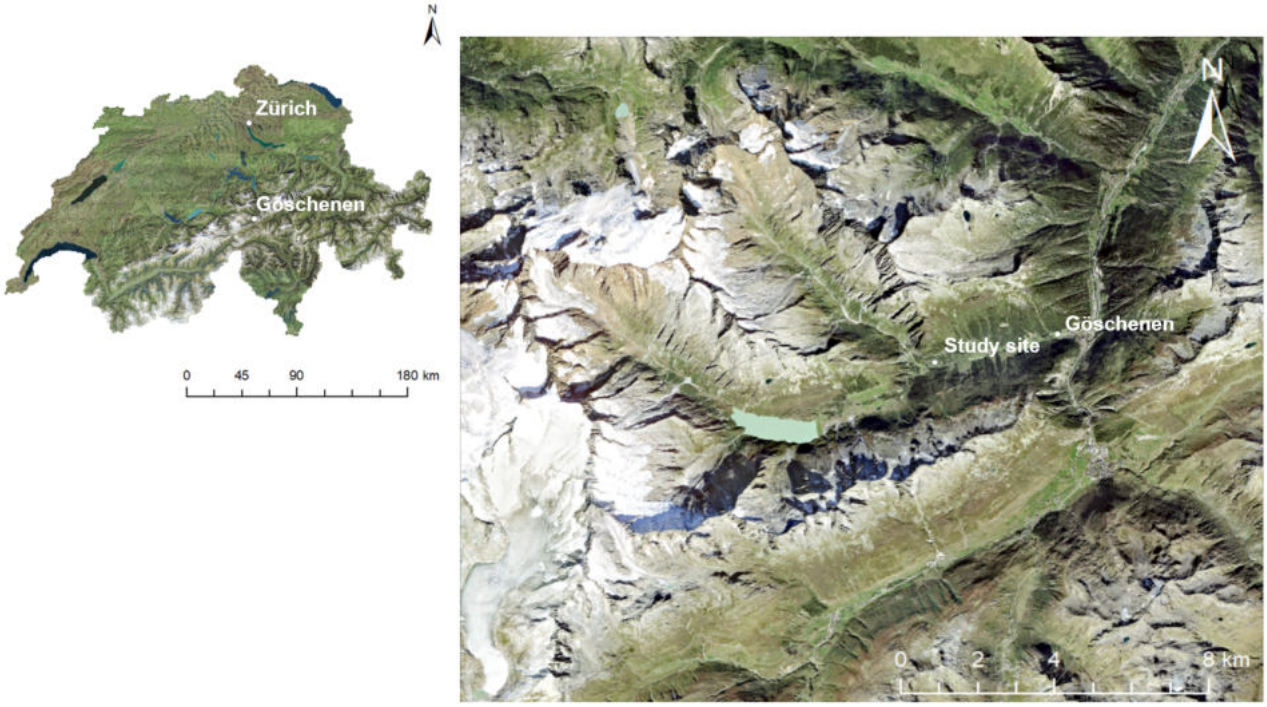

Figure 1: Map and inset map depicting location of the study site in relation to Switzerland (SWISSIMAGE 25 provided by Swisstopo, 2021).

2.1 Location

Located on the north-facing slope in a location called "Sulz", the study site is one of many slopes at the Göscheneralp where snow avalanches and other natural events tend to happen and therefore served as an excellent place for a study. Next to the Sulz slope is "Hutzgen", where possible snow avalanches could also have been affecting Sulz, therefore sometimes also referred to in this thesis. The southern mountain range includes the Dammastock (3630 m.a.s.l.) as the highest point and below it the Damma glacier, serving as an important input of freshwater for the reservoir dam built in the 1960s. The northern mountain range is home to many mountains, such as the Salbitschijen (2986 m.a.s.l), being especially popular among climbers. The Göscheneralpreuss, stemming from the Damma glacier, flows through the valley and at Göschenen joining the Reuss coming from Andermatt.

The elevation of the study site is at around 1250 m.a.s.l., with a gradient of 120 metres from the bottom of the slope to the top, the top being where the last tree was sampled (see figure 12). Situated

Figure 2: Picture taken from below and across the Göscheneralpreuss, showing the study site with the distinctive granite slab.

above the site is a slab of granite rock, with occasional green patches in between. In addition, some small streams are flowing downwards, depending on the hydrological conditions on the site. Next to snow avalanches, rockfall is a prominent feature of the landscape, with many boulders situated in the field. The slope gradient of the slope itself is just below 30°. Above the slope, the gradient changes and is almost always above 30°, therefore, promoting snow avalanches (Schweizer, 2004). At the study site, as well as the whole valley, mostly spruce, larch, birch and mountain pine are growing. Moreover, a whole array of shrubs and other bushes are thriving. Interestingly, many birch trees were growing at the study site. A small plateau can be found above the study site, extending just below the whole southern mountain range. Mostly shrubs thrive there as well as some singular trees, such as mountain pine and some spruce, however soon receding due to the upper forest boundary.

2.2 Climate

The local climate is characterized by about 1500 mm of precipitation per year, which is more than the swiss mean. Nearby, at the Damma glacier, at around 2000 m.a.s.l., the yearly precipitation is higher by around 500mm, which is quite a high gradient of precipitation (Bernasconi et al., 2011; Paul et al., 2012). The mean annual temperatures range around 0 to 5°C in the Göscheneralp (Dümig et al., 2011).

2.3 Geology

The Göscheneralptal belongs tectonically to the "Infrahelveticum" which is made up of crystalline from the Aare massive as well as from autochthonous mesozoic sedimentlayers and some subhelvetic cover

rocks (see figure 3). Mineralogically, the infrahelveticum consist of oldcrystalline gneiss and slate as well as granitic intrusive rock which was formed 300 million years ago. According to the classification, the area between Gurtnellen and Schöllenen up to the Fellital, including the Göscheneralptal and northern Furka region belong to the central Aare granite. The study site is characterized by biotitegranite with some green-colored feldspar (Bernasconi et al., 2011; Spillmann et al., 2011).

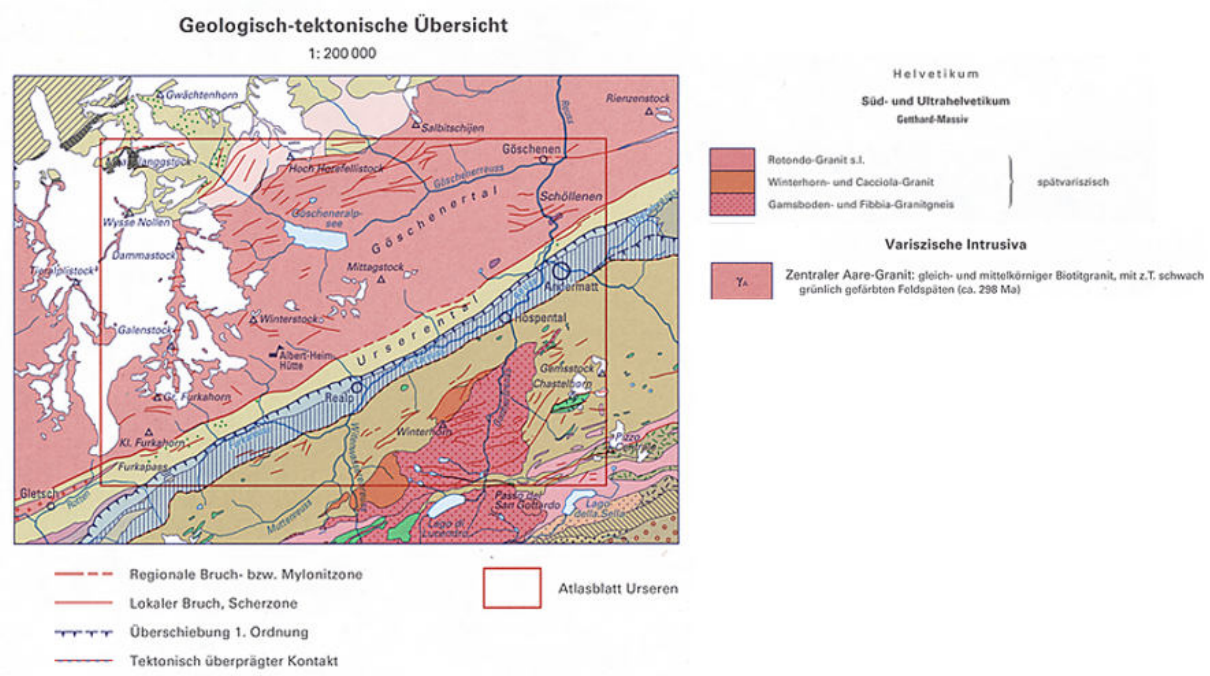

Figure 3: Map and legend of the geology of the Göscheneralp region (map.geo.admin.ch, 2021).

2.4 Snow avalanche records

Snow avalanche records of the area were retrieved on the one hand from the canton Uri, which provide a detailed listing of past events across the whole canton on request. On the other hand by the WSL Institute for Snow and Avalanche Research (SLF), which offered a small Geodatabase of the events at the study site Sulz. Following in table 1, a small register of the events:

Snow avalanche records for the study site			
Year	Event	Date	Information
1951	Sulz	Jan. - Feb.	Snow avalanche winter, multiple ones along the whole valley
1969	Sulz	04.05.1969	Snow avalanche crossing the river and surging 30m high on the opposite slope
1970	Sulz, Hutzgen	10.03.1970	Big snow avalanches at both slopes
1975	Sulz, Hutzgen	06.04.1975	Snow avalanches at both slopes crossing the river and surging 90m high on the opposite slope
1999	Sulz, Göscheneralp	Jan. - Mar.	Snow avalanche winter
2003	Slope opposite Sulz	06.02.2003	Powder avalanche stemming from across Sulz, possible interference
2018	Hutzgen	Jan., Mar.	Possible damages at Sulz from Hutzgen snow avalanches
2019	Sulz	04.04.2019	Snow avalanche without damage to infrastructure
2021	Sulz	April	Big snow avalanche

Table 1: Snow avalanche records of the study site Sulz, and some additional events nearby.

2.5 Tree species

The two main tree species sampled for this thesis were the silver birch (*Betula pendula* Roth) and the mountain pine (*Pinus mugo* Turra).

The silver birch grows all over over Europe and can be found in abundance, due to their thriving seed production. The birch may grow up to 30 m and reach an age of around 90-110 years. Due to its winter hardiness, it can also be found in higher elevations than other deciduous trees, but is vulnerable to colder winds and drought. Moreover, the birch tree is a pioneering species. Therefore, especially during the early stages, it can be found in snow avalanche slopes (Beck et al., 2016). Notable is the striking white bark interspersed with darker querlenticells, this plays a major role in terms of surface temperature of the birch (Roloff et al., 2010).

Figure 4: Silver birch (*B. pendula*)

Figure 5: Mountain pine (*P. mugo*)

The mountain pine, sometimes also dwarf mountain pine, is a rather creeping species. Though it is able to reach heights of up to 5m, usually it is constrained to around 1-2m in growth. The pine may be found predominantly in the Eastern Alps and is endemic to Southern and Central Europe. The species may grow quite old, reaching 150-200 years and in some rare cases even 250-300 years. Branches and trunk are very resistant to cold weather and disturbances such as snow avalanches (Bebi et al., 2009), therefore, also thriving in higher altitudes. In contrast to the green alder (*Alnus viridis* Chaix), which also grows in similar spots (Bühlmann et al., 2014), the mountain pine is preventing soil erosion and serves as protection from snow avalanches. Due to its slim and slow growth it is rarely cultivated (Alexandrov et al., 2019; Monteleone et al., 2006).

3 Theory

3.1 Dendrochronology

The term dendrochronology, sensu stricto, covers all the areas of science where tree rings are used to date wood, as for example in archaeology (Schweingruber, 1996). Coined from the ancient Greek terms dendron (δένδρον – tree), chronos (χρόνος – time), as well as logos (λόγος – science), it is the science of using tree ages.

Before radiocarbon dating became a prominent method for precise age determination, the dating of tree rings was the sole method to determine the age of a tree. With this method, the outermost tree ring is used to date the tree, since it displays the last growth period before felling. Prior to that being discovered, structure and variability of tree rings as well as visible influence of mechanical impacts were studied and described. In the beginning of the 20th century, the American Andrew Ellicott Douglass was the first to establish a method upon realizing there were similarities in tree ring growth in different trees from the same area. As a consequence, he successfully cross-dated a dead stump to nearby trees using his tree ring chronology. It was therefore also possible, to date other trees and events from unidentified ages. In further studies, Douglass successfully extended his tree ring chronology and thus, it was possible to accurately date several sites under examination, such as the famous dating of the Pueblo ruins as well as the Mesa Verde in Colorado. Hence, dendrochronological age determination was accepted as an absolute dating method and still serves as a pillar for age determination in geosciences (Gärtner et al., 2013b; Taylor et al., 1992).

Dendrochronology is often paired with archaeology (for example the age determinations at the neolithic site Pfyn in Niederwil) as well as climate reconstructions. Using tree rings to gather more information of past glacial coverages and fluctuations, remains a vital part of scientific work with tree rings. In addition, dendrochronology is used together with ecology leading to dendroecology, studying the joint effects of tree rings coupled with climate, geomorphology, tectonics, snow mechanisms and other environmental sciences (Gärtner et al., 2013b; Taylor et al., 1992). A more eccentric approach involves the dating of musical instruments. As for example to provide provenance and minimum age of a Stradivari violin, adding to the importance of dendrochronology across all branches (Cherubini, 2021).

3.2 Dendrogeomorphology

Differently to the previously defined term of dendrochronology, morphology, according to the Merriam-Webster Dictionary, is the study of structure and form. Geomorphic mass movements such as landslides, rockfall and soil creep influence growth and vitality of trees. Dendrogeomorphology therefore concerns itself with dendrochronology and plant ecology in combination with geomorphic events (Butler, 1987; Gärtner et al., 2013b).

3.2.1 Trees and disturbances

Common indicators of geomorphic processes are altering the growth, resulting in reaction wood and eccentric growth. Further signs are tilting, scars and injuries, burying and exposure of stem and roots. These disturbances are referred to as growth disturbances and are common in areas with snow avalanches, rockfalls, landslides and other geomorphic events (Stoffel et al., 2014).

Injuries caused by rockfall or snow avalanches may lead to open wounds or even breaking of a branch or stem (see figure 6). The tree reacts by compartmentalizing the wound and the production of callus tissue, overgrowing and closing the wound. Another reaction is the formation of traumatic resin ducts (TRDs). These are tangential rows in which resin is formed. Resin being toxic to fungi and insects as well as having mechanically defensive properties (Krokene et al., 2008). TRDs can be formed quickly and resin transported to the injured part of the tree. The formation of the TRDs may reconstruct disturbance events during the year, this is however contested and not applicable to all tree species, especially with appliance to the growing season (Gärtner et al., 2009; Stoffel et al., 2014). Unfavourable growth conditions may lead to totally, locally or partially missing rings in a tree. Missing rings most frequently originate from drought, however, also stem from late and early frost or heatwaves and can therefore be interpreted as disturbance events stemming from multiple reasons (Bräuning et al., 2016).

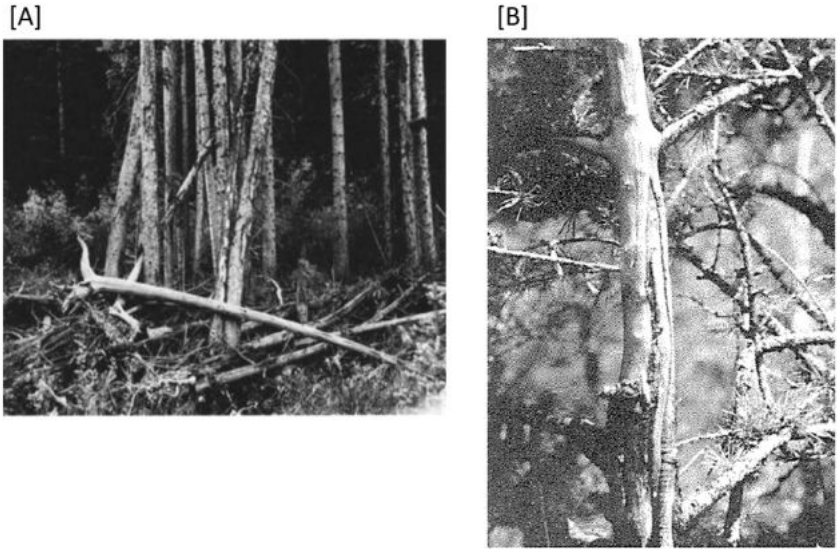

Figure 6: In [A], uprooted and broken trees (Carrara, 1979, p.778). In [B], tree injured by debris or other disturbance (Schweingruber, 1996, p.185).

Trees in the mountains are heavily impacted by snow avalanches, altering growth and vitality of a tree in a long term. Next to snow avalanches, trees may also be impacted by creeping snow or simply snow pressure. Snow avalanche always take place in the dormant season, therefore the disturbances can only

be assessed in the following growing season (Luckman, 2010). Snow avalanches (see also figure 7) often exhibit a strong effect on the function and structural integrity of a forest situated in high mountains. Disturbed forests also have benefits for biodiversity and provide unique habitats, whereas the structure influences the protective qualities (Bebi et al., 2009; Schweingruber, 1996).

Figure 7: Snow avalanche in action at the study site during spring 2021. Video by Seraina Wicky, 2021.

3.3 Tree growth

Trees, in general, tend to exhibit growth by formation of rings. As a differentiation, primary growth is when the stems and roots grow in length. Secondary growth, increase in thickness, is shown to have been developed by trees during the Devonian period, some 400 million years ago. Growth happens in shoot, stem and root usually not at the same time. Starting in the twigs, proceeding to the stem, and then extending to the roots. The cambium (also vascular cambium), which consists of living cells, produces, through cell division, phloem outwards and xylem inwards. The xylem, which acts as wood cells, can then be distinguished as the annual tree growth. This then marks the annual vegetative period, which in the temperate zone restricts from from late spring to fall. Restrictions for tree growth are given by species-specific growth patterns, altitude and geographical location and weather influences, which can be summarized as environmental conditions. Whereas in tropical regions trees tend not to build annual year rings due to almost non-existent seasonality, in temperate to dry climates seasonality leads to the formation of annual rings. (Butler, 1987; Fritts, 1976a; Gärtner et al., 2013b; Schweingruber, 1996; Stoffel et al., 2008).

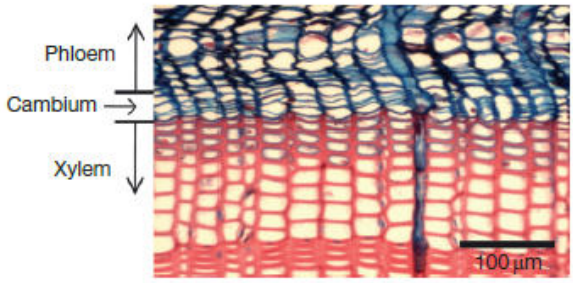

Figure 8: Thin section depicting the cambium as well as phloem growing towards bark and xylem growing towards pith (Gärtner et al., 2013b, p.92).

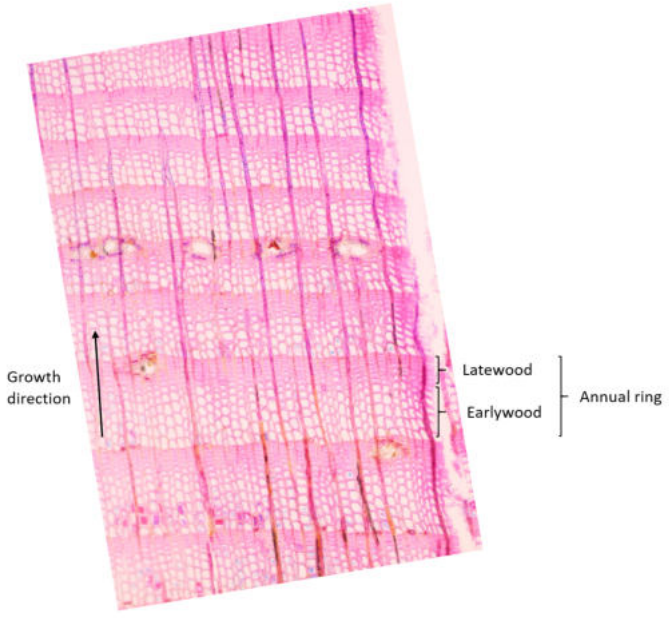

Figure 9: Thin section of Larch (*Larix decidua* Mill.) showing early- and latewood in annual rings.

Trees form different amounts and sizes of cells during the vegetative period. Conifers are producing larger tracheids during the start and get smaller to the end of the vegetation period, also exhibiting thicker tracheid walls. In angiosperms, tracheids are larger in the beginning of the vegetative period and get smaller to the end of it. This difference in size and thickness of tracheids can be differentiated into earlywood and latewood. The former growing during the spring and early summer months, whereas the latter builds up in late summer and fall. Earlywood cells, with their larger lumen and smaller cell wall thickness, are responsible for the nutrient and water transport. Latewood cells, with their smaller lumen and much thicker cell walls, contribute mainly to the stability of the tree. The size of the

cells in the cambium is influenced by ecological conditions such as weather (Gärtner et al., 2013b; Rathgeber et al., 2016; Schweingruber, 1996; Smith, 2008).

Trees growth also depends on the environmental conditions. On the one hand, the tree is responsive to the energy and water balance given at a particular location. Changes to these long-term balances affect the tree and can be inferred from tree-rings. Furthermore, site-specific factors such as topography, substrate, elevation and orographic exposure influence the individual tree growth to a large extent. For example, in alpine environments, the temperature acts as a limiting factor, having an impact on the length of the growing season (Carrer et al., 2007). On the other hand, biotic influences stemming from living organisms also shape the growth of a tree. Lastly, climate influences the long-term growth and the frame conditions of tree growth from early on (Fritts, 1976b).

3.3.1 Reaction wood

When a tree is disturbed, for example tilted or bent, the tree reacts by forming reaction wood, in order to regain its vertical position. This is tension wood in angiosperms and compression wood in gymnosperms (Schweingruber, 1988; Stoffel et al., 2008; Wilson et al., 1977).

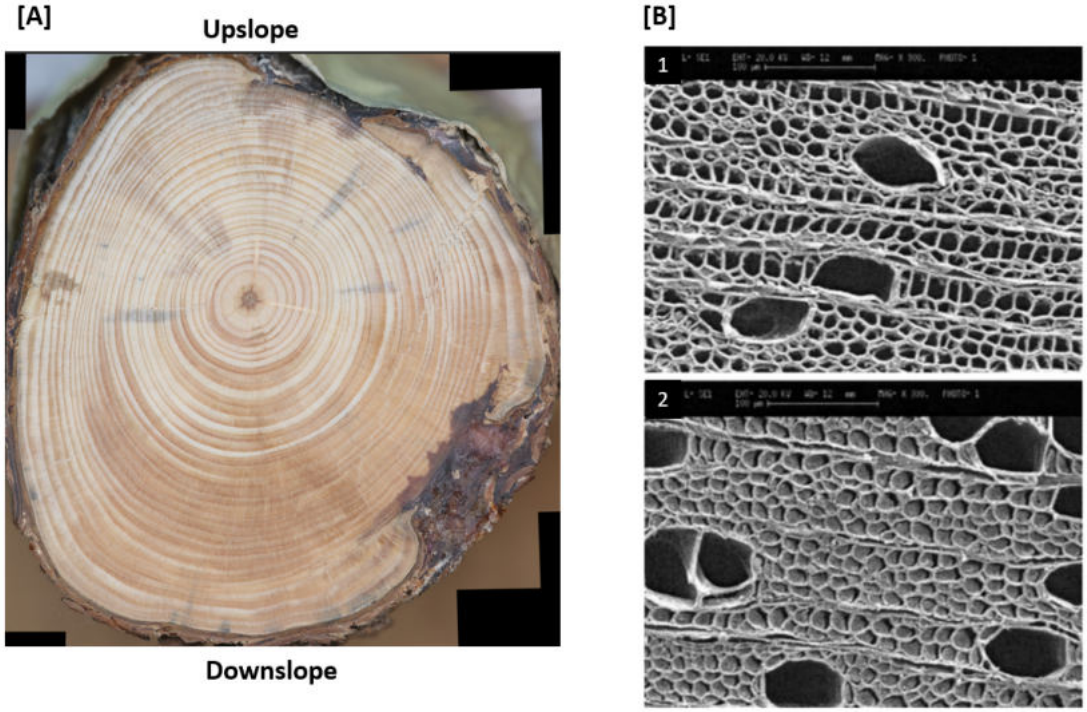

Figure 10: In [A], compression wood of mountain pine (P. montana), distinctly visible on the lower side of the disc. In [B], image of Poplar species showing normal wood (1) as well as tension wood (2) after Coutand et al., 2004, p.21.

Deciduous trees form a larger ring on the upper side of the direction in which the trunk is tilted to, pulling themselves upright. This tension wood is only distinguishable on cross-sections by a sheen

from normal wood. Also, most angiosperms produce a gelationous layer (G-layer) inside the fiber cells, better discriminable from normal wood. If the G-layer is not present, increased cell-wall thickness and different anatomical structures of the entire ring are exhibited. Since the identification and recognizing of tension wood in angiosperms is challenging and labour intensive, most reconstructions of events are done with species that display compression wood (Gärtner et al., 2013b).

Heinrich et al. (2008) bent two angiosperms species mechanically to different angles and examined the effects in the tension wood. The more bent the tree was, the more intense tension wood was formed. Additionally, growth increments on the opposite side were also smaller than in less bent trees, leading to even more eccentric growth. Differently to tension wood, compression wood is formed on the lower side of the tilted trunk, pushing themselves upright. Cell walls are much thicker as well as more roundly shaped. Normal cells,in comparison, show larger intercellular spaces and are more quadratically shaped. This appears in often larger and darker compression wood rings for years with lots of disturbances (Carrara, 1979; Gärtner et al., 2013b; Schweingruber, 1996; Wilson et al., 1977). Mostly, reaction wood is used to date disturbance events, however it cannot be definitely determined if the reaction is from the actual year of the disturbance, since damages may remain for years after the event. Furthermore, several events per year cannot be established by the intensity of the reaction wood (Casteller et al., 2007). Another reaction to a disturbance event may be that the tree growth reduces, possibly due to the damage of roots (Stoffel et al., 2008).

3.3.2 Eccentricity

As stated in chapter 3.3.1, a tilted tree is always going to try to regain its vertical position through reaction wood. As an effect, tree growth changes from concentric to eccentric growth. Eccentricity being characterized by producing wider rings on one side of the stem than on the other one (Figure 11)(Braam et al., 1987). Usually, other methods such as the dating of dead trees, identifying of minimum age and analysis of wood anatomy of disturbed trees come at hand at identifying geomorphic events. More often, the classic method of reaction wood is applied for dating such an event. Tree ring eccentricity can give an overview over single events of geomorphic events such as a landslide (Burkhalter et al., 2019; Malik et al., 2016). Furthermore, using eccentricity in landslide analysis, as a method to detect past events, appears to be a sensitive method (Šilhán, 2019). In a study set in a dune setting, Koprowski et al. (2010) showed that in sand burial of Scots pine (*Pinus sylvestris* L.), trees showed eccentricity years ahead of compression wood formation. Therefore, suggesting that eccentricity may be more sensitive to disturbances such as sand invasion.

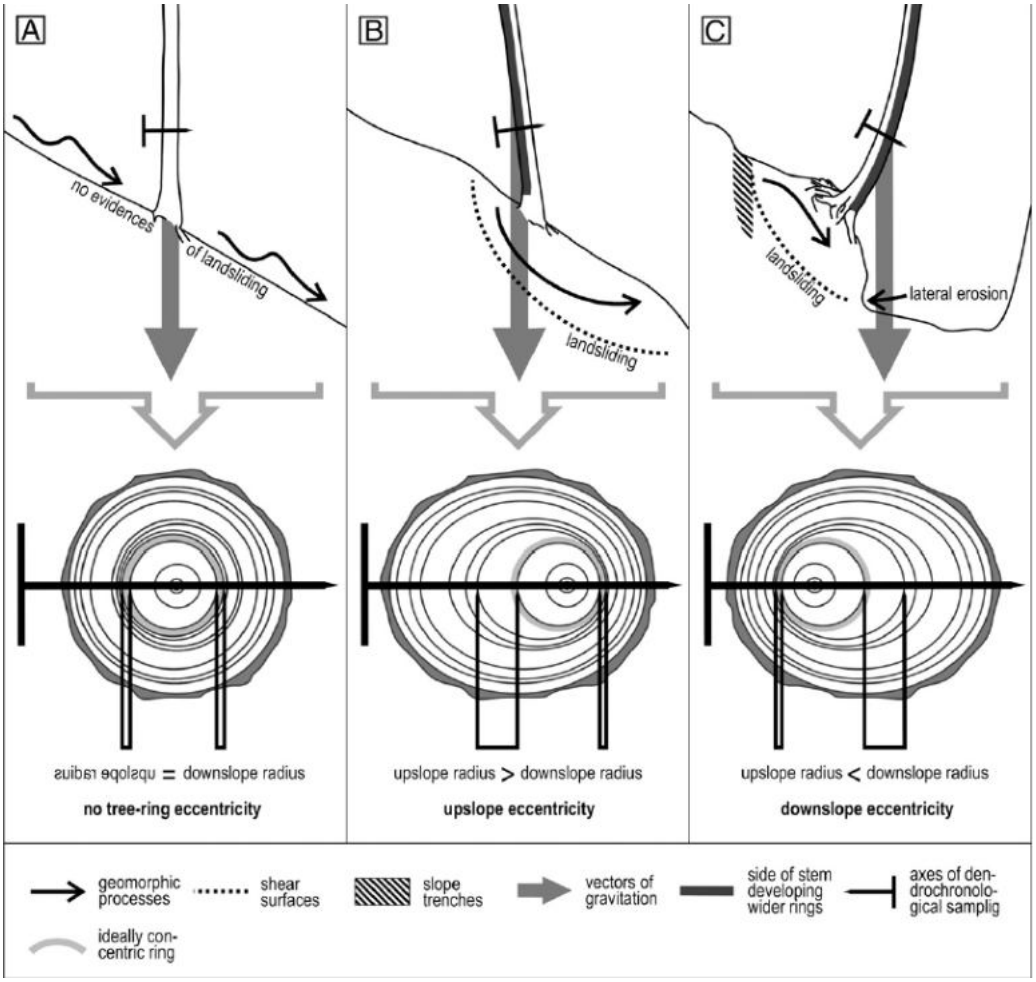

Figure 11: Eccentricity in trees due to different geomorphic processes. In [A] no eccentricity, in [B] upslope eccentricity due to reaction wood on upper side, and in [C] downslope eccentricity due to reaction wood on lower side of stem (Wistuba et al., 2013, p. 47).

Eccentric growth in trees has many sources, also occurring all at once. The impact of snow avalanches, creeping snow as well as general snow pressure, exert a force on the tree, leading to eccentricity in trees (Schweingruber, 1996; Wistuba et al., 2013). Studies involving eccentricity for snow avalanches have been done by Casteller et al. (2007), where for prominent snow avalanche years the eccentricity before and after were compared and events and areas of snow avalanches were determined by also using reaction wood. Additional studies have been done using eccentricity in combination with other dendrochronological dating methods to date past snow avalanches (Casteller et al., 2008) and as a help to distinguish growth disturbances and avalanche activity (Decaulne et al., 2011). Also, wind can induce stem eccentricity, different to eccentricity in a landslide, by physiologically altering tree growth as well as showing different patterns by shifting the direction of eccentricity during the years (Wistuba et al., 2018).

3.3.3 Eccentricity indices

For this thesis, eccentricity indices were taken directly from Wistuba et al. (2012). These indices have been used to date landslides and not snow avalanches. However, this approach was used since it does distinguish between upslope and downslope eccentricity, as well as giving eccentricity values in percent change. Other studies, such as Casteller et al. (2007), only show eccentricity changes before and after a snow avalanche event. Hereinafter, the eccentricity indices used will be explained. In (1), a simple eccentricity index (*Ex*) of a tree ring is depicted:

$$Ex(mm) = Ux - Dx \tag{1}$$

For each equation x stands for the annual tree ring. Downslope (Dx) radii are subtracted from upslope (Ux) radii. If the upslope radii are larger (>0), upslope eccentricity is assumed. If the downslope radii are larger (<0), downslope eccentricity is assumed. Given that the value of Ex is > 0, eccentricity index of a tree ring (2) in % is given by dividing Ex by Dx and multiplying by the factor 100, in order to have percentage change. Given that the value of Ex is < 0, eccentricity of a tree ring (3), in % is given by dividing Ex by Ux and multiplying by the factor 100, in order to have percentage change.

$$Eix(\%) = (Ex/Dx) * 100\% > 0, \tag{2}$$

$$Eix(\%) = (Ex/Ux) * 100\% < 0, \tag{3}$$

$$Eix(\%) = Ex(mm) = 0, \tag{4}$$

both upslope and downslope eccentricity index in (2) and (3) are explained in relation to the narrower part of the respective radii. A lack of eccentricity (4) is assumed if *Ex=0*.

In order to obtain values for yearly change and to date snow avalanches, the difference between the eccentricity index (*Eix*) values for a tree ring in a certain year and the year before was calculated in (5):

$$vEix(\%) = Eix - Eix - 1 \tag{5}$$

4 Material and methods

The sampling of the trees represent the fundamental work of this thesis. The following chapter describes the sampling as well as giving information on quantity, quality and preparation of the samples for the analysis. Next to that, methods that were used to analyze the data are described. Guidelines were given by Stoffel et al. (2008), Schweingruber (1988) and (Gärtner et al., 2013a).

4.1 Sampling

4.1.1 Samples

The sampling of the trees took place in mid-August and required five days in total. Depicted in table 2 are all the samples of disturbed trees which were extracted. Since taking samples from trees influenced by geomorphic events, the pith is placed and, therefore, taking a perfect sample is much harder (Wistuba et al., 2012). Cores were extracted with an increment corer (5 mm), discs with a handsaw.

Type	Alive	Dead	Tree species	Year	Total
Cores	54	0	Birch	2021	54
Disks	40	1	Mountain pine	2021	41

Table 2: Samples taken from disturbed trees during the sampling trips.

Per disturbed birch tree, two cores were extracted at a height of ca. 1.30m, one from the downslope side as well as from the opposite upslope side. This was done in order to get the tilting event, hence it being the axis of tilting. In total, 27 birch trees were sampled with a total of 54 cores. For the mountain pine, cross-sections were extracted, this due to the fact that taking an increment core often was not possible due to the rather slim growth. Also, since the mountain pine grows in branches, usually one bigger branch was sawn off and from there sometimes multiple discs were taken. This was done since it often displayed multiple injuries, which were interesting to date. This amounts to a total of 26 different mountain pine tree, rendering the total number of discs from mountain pine to 41.

Trees in the field were chosen according to visible injuries and also to cover a wide area of the slope. As can be seen in figure 12, many samples are grouped together on the eastern and northern part of the map. This is due to the fact that both groups bore many injuries and were obviously tilted by a recent snow avalanche event. Next to samples retrieved from disturbed trees, reference trees were cored. For the birch, 20 references were cored. Reference trees were sampled perpendicularly to the slope at a height of ca. 1.30m, with two cores each from the opposite side. This was done in order to get as little disruption of growth as possible. Given that undisturbed mountain pines are difficult to locate, undisturbed Norway spruces (*Picea Abies* (L.) H. Karst) were taken and used to cross-date the mountain pine samples. A total amount of 20 reference spruces were sampled the same way as the

birch reference. Reference trees were particularly selected if they bore no visible injuries and preferably older trees were sampled, the latter however is visibly often not as easy to determine (Gärtner et al., 2013a; Stoffel et al., 2008).

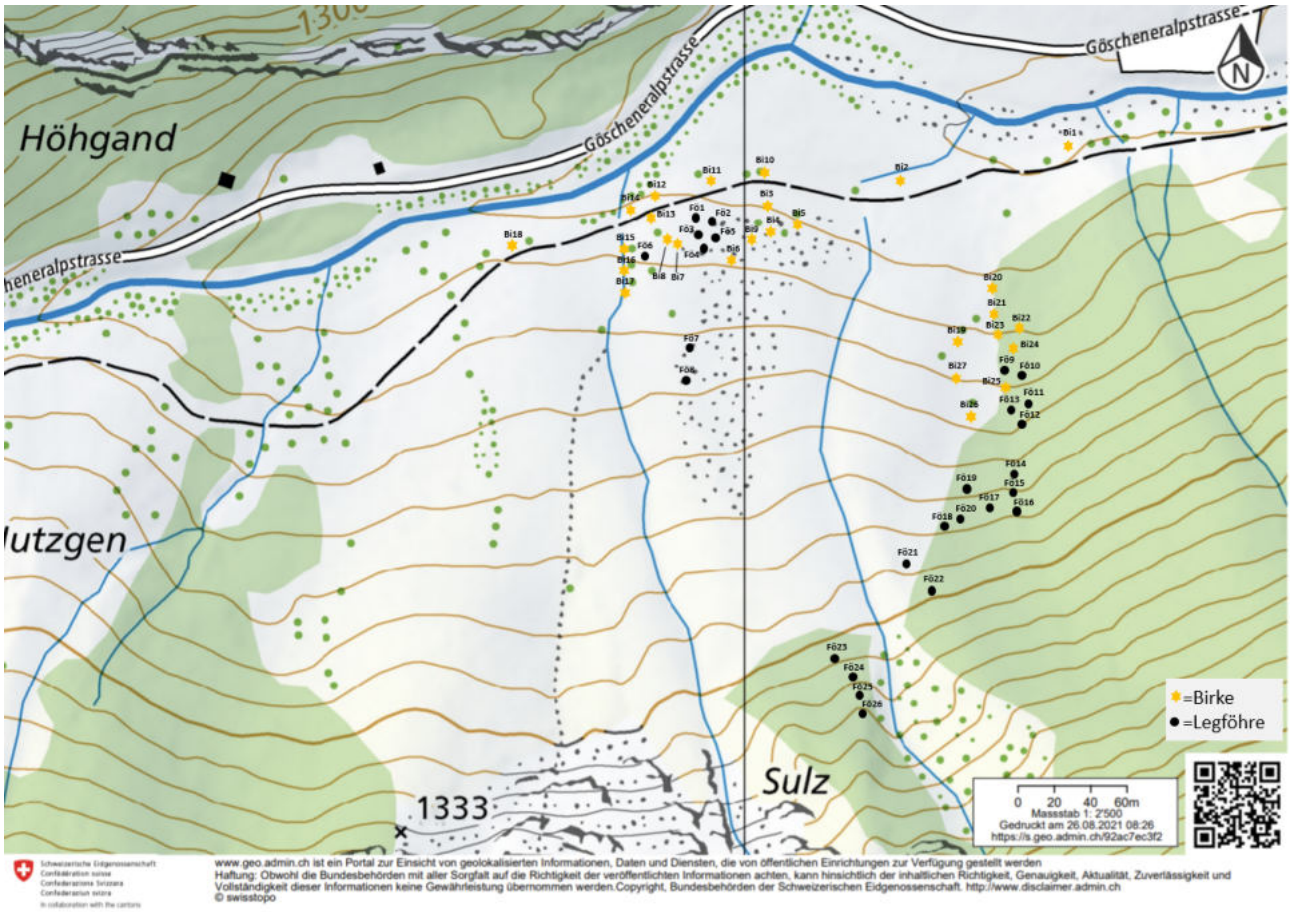

Figure 12: Location of samples distributed at the study site. Yellow stars represent birch trees, whilst black dots depict mountain pine trees (map.geo.admin.ch, 2021).

It is suggested by Schweingruber (1996) to include as least 15 trees in order to get a good reference, therefore, 20 samples were taken. In figure 44 in the *appendix*, time line diagrams of the samples extracted from the birch and mountain pine are displayed. Each bar represents one tree as well as the dated age. For the birch, the oldest tree is dated back to 1986, whereas the oldest pine dates back to 1963. This shows that the series are quite young. For the analysis, not all cores and discs were used, since some of them either were of bad quality and/or impossible to date. Therefore, the actual number of samples used for the analysis is slightly below the quoted values from above.

4.2 Sample preparation

In order to obtain the age of the individual samples, they first needed to be prepared for analysis. This section entails the preparation of the increment cores from birch as well as the discs retrieved from pine, as well as the creation of thin sections. Steps were executed according given to guidance (Gärtner et al., 2013a).

4.2.1 Core and disc preparation

After the core samples were obtained with the increment corer, they were first dried in paper straws, in order to prevent rotting. Following that, they were placed in plastic holders and labelled accordingly. The discs were air dried and then labelled on one side.

Figure 13: Labelled core samples placed in plastic holder.

After that, the discs were sanded with sandpaper with decreasing roughness (60 to 320). Thus, the discs surface was very smooth and the rings could be seen clearly. Generally, the cores are glued to a wooden support and then measured with a tree ring width program (Schweingruber, 1988). For this thesis, the cores were first mounted onto the core-microtome. The core-microtome is a device, which was invented at the Swiss federal institute for forest, snow and landscape research (WSL) to enhance the visualization of anatomical properties of wood cores as well as to establish an alternative to the classic sanding method (see figures 14 and 15). The core-microtome is equipped with a blade holder in which a blade can be fixed and with which very thin (10-20 μm) sections of up to 40 cm in length can be cut. This is done by firstly fixing the core to a mount and placing the blade in an angle of around 45° to the core, then the mount can be slightly lifted in 10-20 μm steps. With that, layers of wood can be cut away until the surface is as desired. Since the birch samples used in this thesis exhibit bad contrast, chalk was added in order to increase the latter. This was done by rubbing the chalk onto the surface, which had the effect that the cell lumina were filled up and the cell walls stayed visibly dark. A big advantage of the core-microtome is that the cells of the wood sample are not getting filled up with swath (as in sanding), as well as having a flat surface (Gärtner et al., 2013a; Gärtner et al., 2010).

Figure 14: Mounted core on the core-microtome.

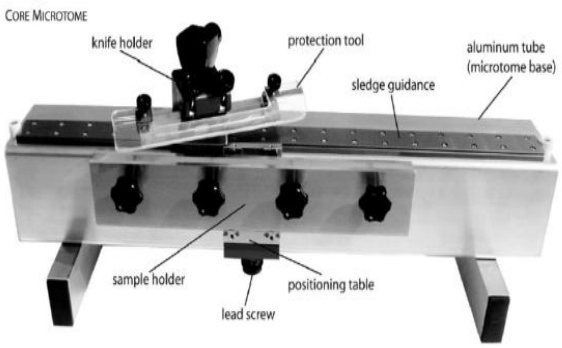

Figure 15: The core-microtome and its features in detail (Gärtner et al., 2010, p.86).

4.3 Thin sections

Tension wood, as already stated in chapter 3.3.1, is hard to identify without producing a thin section, a microscopic slice of the wood sample usually between 10 and 20 μm in thickness. With this method, the anatomical features such as the cells and cell boundaries can be examined in detail (Gärtner et al., 2013b). The first step in obtaining a thin section, is to split the core into smaller parts. Then, a lab-microtome can be used to produce 10-20 μm sections. This because the smaller the core, the easier it is to produce such a section (Gärtner et al., 2013a). From there on, a thin slice is extracted similarly as described in chapter 4.2.1 with the core-microtome. After the thin section is placed upon a glass carrier, glycerin is added in order to prevent the drying of the sample.

Figure 16: Equipment used to stain and rinse a thin section.

From there on, the thin section can be stained in the laboratory chapel shown in figure 16. Firstly,

the thin section is covered with a dye-mix of safranin (staining the lignin red) and astra blue (staining the cellulose blue). After some minutes, the dye is carefully removed with a pipette and tap water. Secondly, 75% ethanol is used to rinse more dye and water from the section. Followed by 96% ethanol and ethanol anhydrous respectively. Thirdly, xylol is added, in order to rinse out the leftover alcohol. As a last step, Canada balm is added. This is done because it preserves and fixates the sample for a long time. Given all these steps were done carefully, a glass cover is placed on top of the thin section and cautiously pressed onto the sample - successfully driving out air bubbles. In an ultimate step, the samples are placed in an oven (60°C) for the purpose of drying. After 24-48 h the sample may be removed from the oven and be reviewed under a microscope. Sometimes some Canada balm has to be scraped of the glass so that a clear view is given (Gärtner et al., 2013a). Thin section can also be scanned with a special scanner made for anatomical analysis. The thin sections created in this thesis will be reviewed in the results section .

4.4 Measurement

The step after preparation is done is to measure the tree-ring widths. For this reason the samples first have to be digitally available. This sections explains the measurement of tree-ring widths.

4.4.1 Skippy

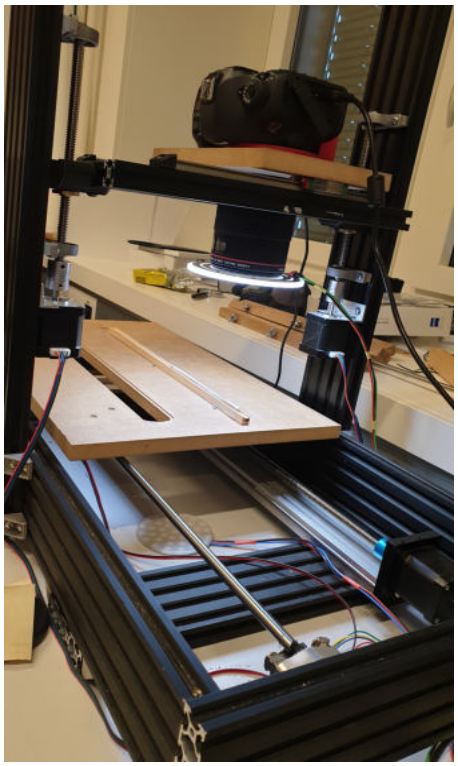

Figure 17: Picture of Skippy at the WSL.

After the sanding of the discs and the cutting of the cores was done, the samples were photographed using Skippy (see figure 17). This prototyp was developed at the WSL by Loïc Schneider and Holger Gärtner and is used to make multiple pictures of samples which can then be stitched together. A camera (here a Canon SLR) is mounted atop a frame. The core can then be placed on the moving platform. By help of a program of the same name, a picture can then be taken each x spacing and subsequently each picture can be stitched together (see figure 18), using a program such as PTGui.

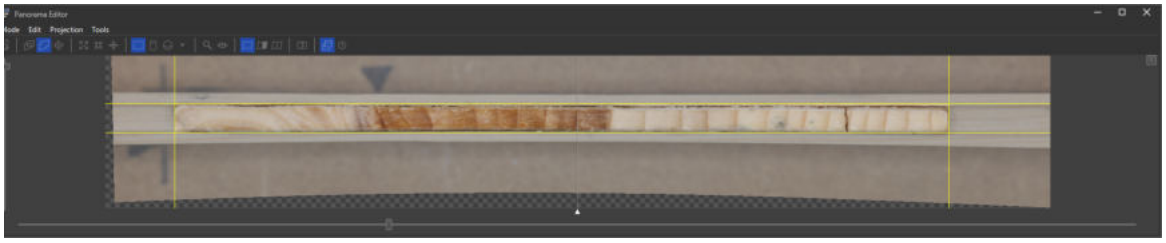

Figure 18: Stitching together the core in PTGui.

4.4.2 CooRecorder

Figure 19: Screenshot of CooRecorder displaying a mountain pine sample with the tree rings distributed.

The measurement of the rings was done using the tree-ring width measurement software "CooRecorder" by Cybis Elektronik Data AB. The analysis of the tree rings is the fundamental work of many dendrochronological studies and therefore indispensable (Speer, 2009). CooRecorder offers a high-

resolution image analysis with an intuitive placement of rings for discs and cores (Maxwell et al., 2021). An image, such as the stitched image from figure 18, can be loaded into the program. From there on, the image resolution can be calibrated via a beforehand prepared calibration sheet. Ensuing, rings can be placed according to the corresponding year-ring boundaries (see figure 19). This results in a .pos-file, which holds the placements of the rings in connection to the image. Next to placement, CooRecorder also offers some options of comparison between cores of a tree and displaying some statistics such as the "Gleichläufigkeit" and a t-value.

4.5 Cross-dating

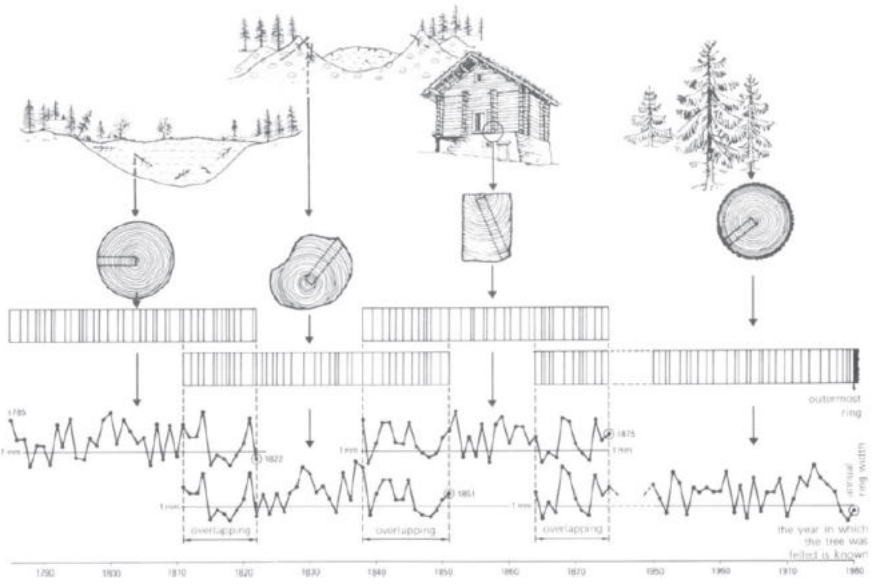

Figure 20: Schematic of cross-dating different trees. By use of bridging technique, different trees can be linked together into a chronology (Schweingruber, 1988, p. 51).

Cross-dating of trees was done after the tree-ring widths of each tree were recorded by CooRecorder. Generally, a sample of unknown age is dated against a master chronology, in which then visually and statistically the sample can be cross-dated into relation. As for example depicted in the classic portrayal in figure 20. Measured tree-ring widths are overlapping with a known chronology and, therefore, can be assigned correctly, also known as bridging technique (Schweingruber, 1988). In this thesis, rather than comparing samples to a known existing master chronology, samples were cross-dated among each other as well as to the obtained reference chronologies.

The analysis of the tree-ring widths was done with TSAP-WIN, a software programme made for that purpose, mainly used here to graphically compare the curves visually for "Gleichläufigkeit" (see figure 21). Missing rings were inserted where necessary in CooRecorder and then checked again in TSAP-WIN. Due to the trees at the study site being rather young, cross-dating with the common methods is rather not suggested. For example, the oldest sample in the birch reference is dated to 1953, which is a rather young timeseries. For the disturbed birch trees the oldest tree is dated to 1986, whereas

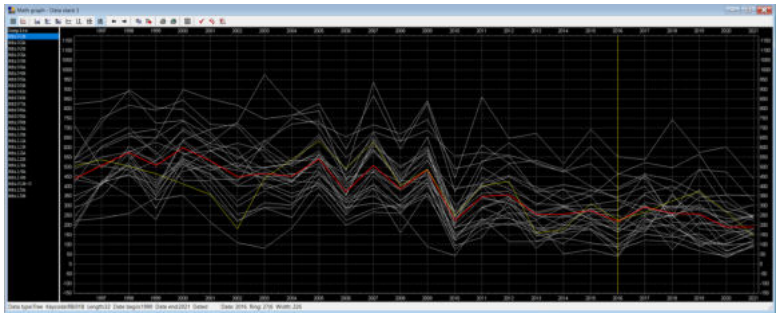

Figure 21: Plot of mean birch reference trees displayed in TSAP-WIN.

in the mountain pine samples, 1963 is the oldest. Longer timeseries are beneficial for cross-dating of trees, generally long-lived species are used for that purpose. Young trees are more often influenced by environmental conditions and, therefore, more erratic and much harder to crossdate, often also due to very irregular ring-width characteristics (Bätz et al., 2016; Tonelli et al., 2020).

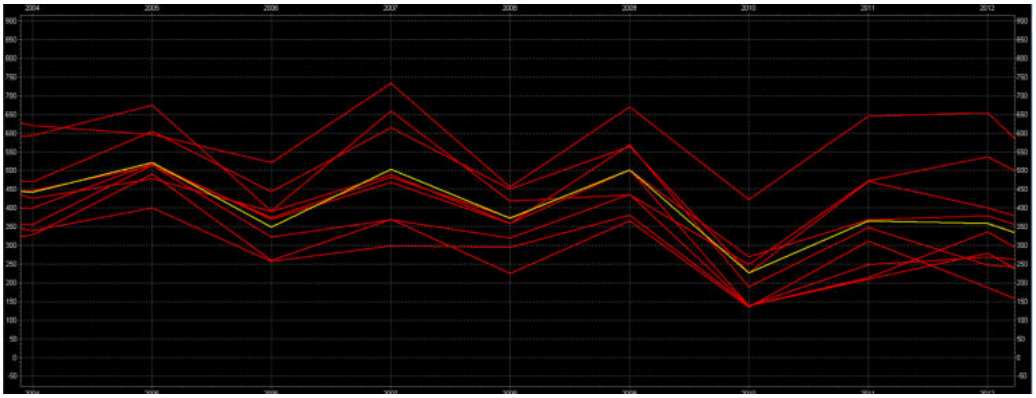

Figure 22: Close-up of several mean reference birch tree exhibiting "Gleichläufigkeit" in years 2006-2010. The yellow line is the overall mean of the reference birch trees.

In their paper, Tonelli et al. (2020) worked with 734 young European black pines (*Pinus nigra* Arnold) with a similar tree age range (1960-2015) as in this thesis. For given trees, statistical parameters were calculated and two methods to test cross-correlation were applied. They concluded that even though it was possible to cross-correlate a large part of the samples correctly (47%), many samples had to be discarded. Further, they add that in order to get a good result a high number of individuals should be sampled. For example, in one site composing the whole dataset, only 8 out of 20 trees were selected due to bad inter-correlation. Since this thesis only concerns with few samples as well as generally very young individuals, trees were cross-dated visually. This is shown in figure 22, where a visual "Gleichläufigkeit" was achieved for nearly all of the sampled trees of the birch reference (here only a small selection). This was also done for the other samples, since the problem persisted to be the same. One possible approach could have been to compare intra-annual density curves to each other, as has been shown to be successful in cross-dating young trees (Raden et al., 2020), this would however have been quite laborious and possibly go beyond the scope of this thesis.

4.6 Eccentricity and threshold calculation

The thresholds for the eccentricity values were set as follows, a total of six different thresholds were calculated, as displayed in table 3. Firstly, the same formula as in chapter 3.3.3 were used in order to calculate *Ex*, *Eix* and *vEix*. For threshold 1 & 2, cores A and B were taken as upslope and downslope respectively. Core B was taken as *Ux*, whereas A was taken as *Dx* in order to get *Ex*. From there on, *Eix* and *vEix* were calculated via the formula. Threshold 1 uses the mean of all years of *vEix* in order to get positive/negative values. A column with positive and negative means was formed, from which on the mean of all those values was computed. The final value was then calculated by either adding the standard deviation to the positive mean or subtracting the standard deviation from the negative mean. This resulted in either a positive or negative value per year. Threshold 2 uses the same calculation as threshold 1, with the exception that not the mean but the median was calculated. This too then resulted in the creation of one positive/negative value per year. After that, the positive and negative values from each year were summed up, which resulted in one mean value for each positive and negative. The appendix includes the calculation of the eccentricity in Microsoft Excel. This might serve as a better understanding.

Threshold 3 & 4 were calculated in the same manner as the previous two thresholds were. Threshold 3 also was calculated via the mean whereas for threshold 4, the median was calculated. The only exception is that for the calculation of *Ex*, core A and B were flipped, meaning upslope and downslope were reversed, which resulted in different values.

Number	Positive [%]	Negative [%]	Calculation Type
Threshold 1	56.78	-59.43	mean
Threshold 2	51.81	-45.90	median
Threshold 3	65.33	-50.31	mean
Threshold 4	40.98	-46.22	median
Threshold 5	29.57	-33.98	first quartile (Q1)
Threshold 6	31.56	-32.57	third quartile (Q3)

Table 3: Different thresholds that were calculated. The last column shows how the data from *vEix* was calculated in order to get the values.

Finally, threshold 5 & 6 were calculated by also using the values for *Ex* from thresholds 1 & 2. Instead of utilizing the mean and median of *vEix*, quartiles were taken. For threshold 5, the lower quartile (Q1) of the values was taken. This means that 25% of the data is smaller than this value, the value is defined between the median as well as the smallest observation of the data. For threshold 6, the third quartile (Q3) of the values was taken. This means that 75% of the data is smaller than this value. It is calculated to be between the highest number and the median of the data. Those two measures were taken since it provides a certain overview over the range of the data.

The eccentricity values from the birch trees were calculated with the formula presented in chapter 3.3.3. Accordingly, values for *Ex*, *Eix* and finally *vEix* were computed. In a next step, each value (in

%) for each year and tree was tested to be either above or below the specified threshold. If one or the other was true, an eccentricity event was noted and and marked with either negative or positive eccentricity. This is presented fully in the *results* chapter, in figures 23, 24 and 25. Additionally, means of yearly *vEix* values of trees were taken (if at least 3 observations) and the same thresholds as above were applied. This resulted in figures 26, 27 and 28. In contrast to applying the threshold to each *vEix* value from each tree for each year, this approach applies the threshold visually to the mean curves for the eccentricity values per year.

5 Results

The following section will present the results obtained by the analysis of the samples. Not all the plots and data are shown here, for more see the *appendix* at the end of this thesis.

5.1 Eccentricity figures

This section shows the birch eccentricity plots which were produced with R Studio (RStudioTeam, 2020). A more detailed explanation of the calculation can be found in chapter 4.6 as well as some theory in chapter 3.3.2. In the three following figures, eccentricity events exceeding the respective thresholds are presented. An event was noted if it was larger respectively smaller than the specified thresholds. On the x-axis the years are depicted, whereas on the y-axis the number of events are shown. For each year, two bar graphs are plotted showing upslope (red, left-side) and downslope (blue, right-side) eccentricity. In total 23 birch trees were used with the oldest tree dated back to 1986. Below each graph, above the x-axis, the number of trees per year is depicted.

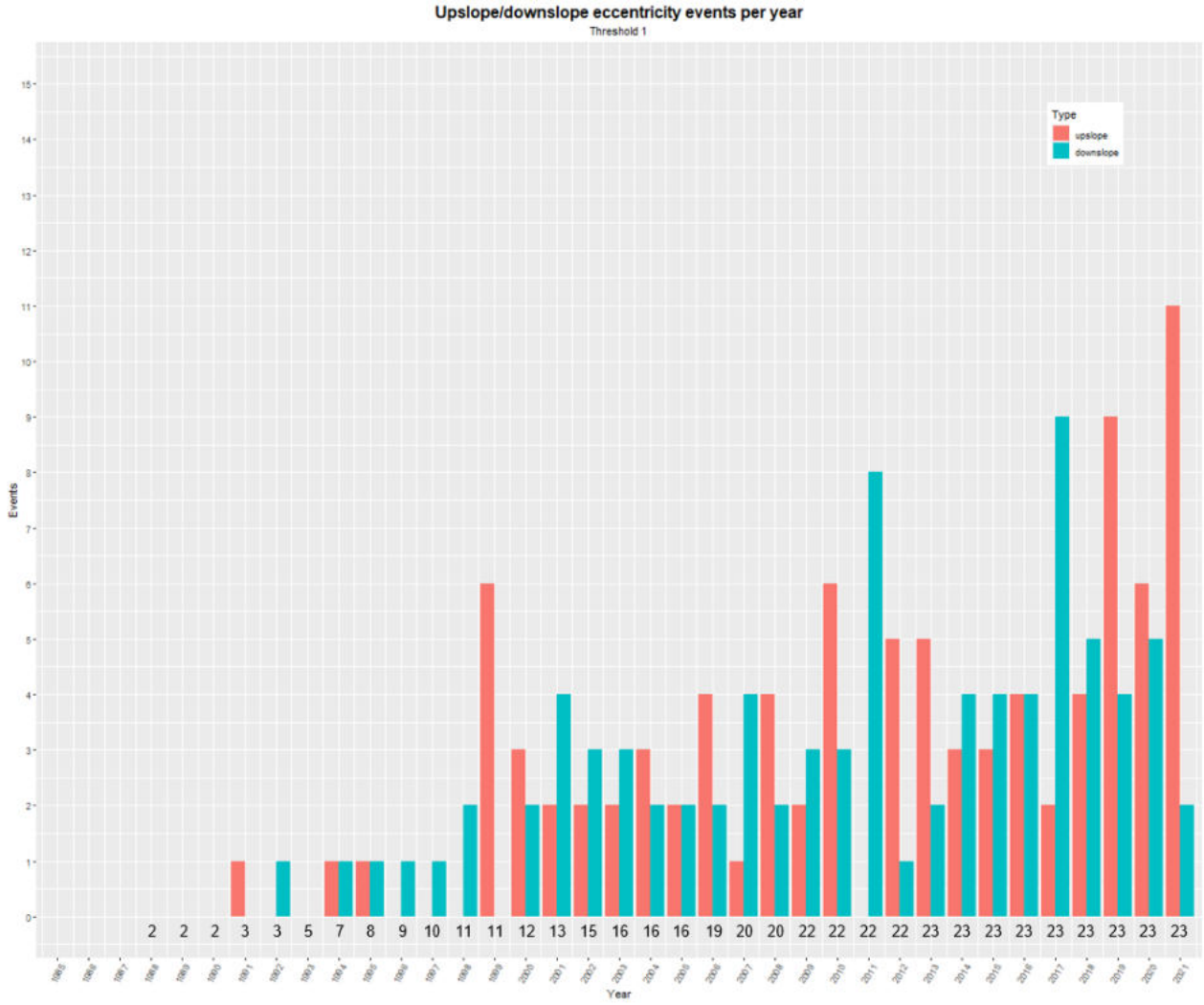

Figure 23: Eccentricity events in sampled birch trees exceeding threshold 1.

Above in figure 23, eccentricity events exceeding threshold 1 are depicted. The oldest event was dated to 1991. For the 23 trees used in the analysis, there is not always a signal exceeding the threshold. Overall there are less events from 2000-2005 and from 2013-2016. Since disturbed birch trees exhibit tension wood, upslope events are looked at specifically. Clear signals, meaning spikes in upslope values, can be assessed in years 1999, 2000, 2006, 2008, 2010, 2012-2013 and 2019-2021. Large spikes in downslope events can be seen in years 2001-2003, 2007, 2011, 2017-2018. Particularly large upslope events are in 1999, 2010, 2019 and 2021, whereas particularly large downslope events are in 2011 and 2017.

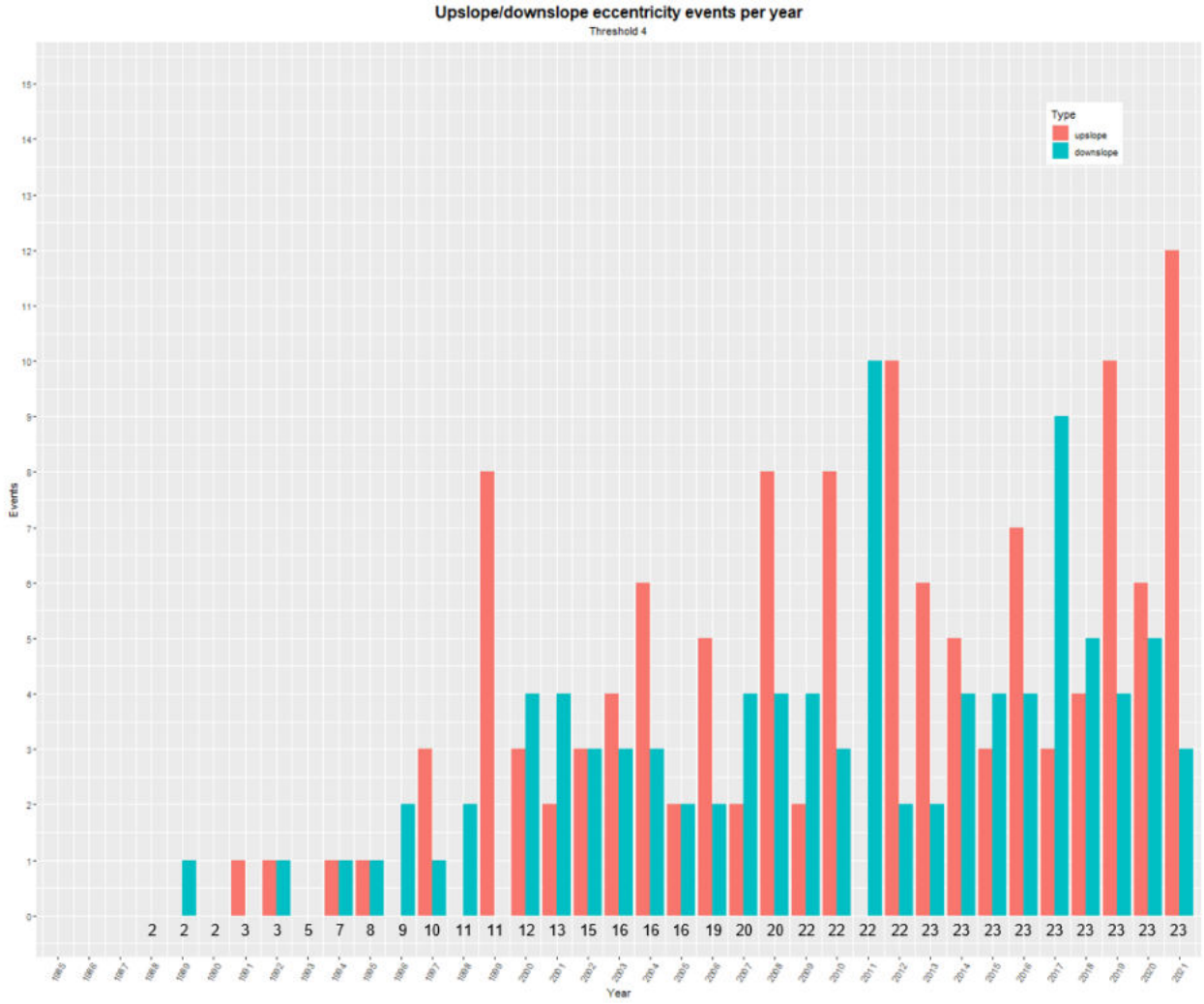

Figure 24: Eccentricity events in sampled birch trees exceeding threshold 4.

In figure 24, events are displayed exceeding threshold 4. The positive/negative threshold is markedly smaller than depicted in the previous figure (see table 3). The oldest dated event is listed in 1989, with the oldest tree dating back to 1986. A trend is harder to spot but noticeably more upslope events are shown. Many upslope events can be noted in years 1999, 2003-2004, 2006, 2008, 2010, 2012-2013, 2016 as well as from 2019-2021. Downslope events are numerous in years 2001, 2007, 2011 and 2017. In particular large upslope bars can be seen in 1999, 2008, 2010, 2012, 2021 while many downslope events happened in 2011 and 2017.

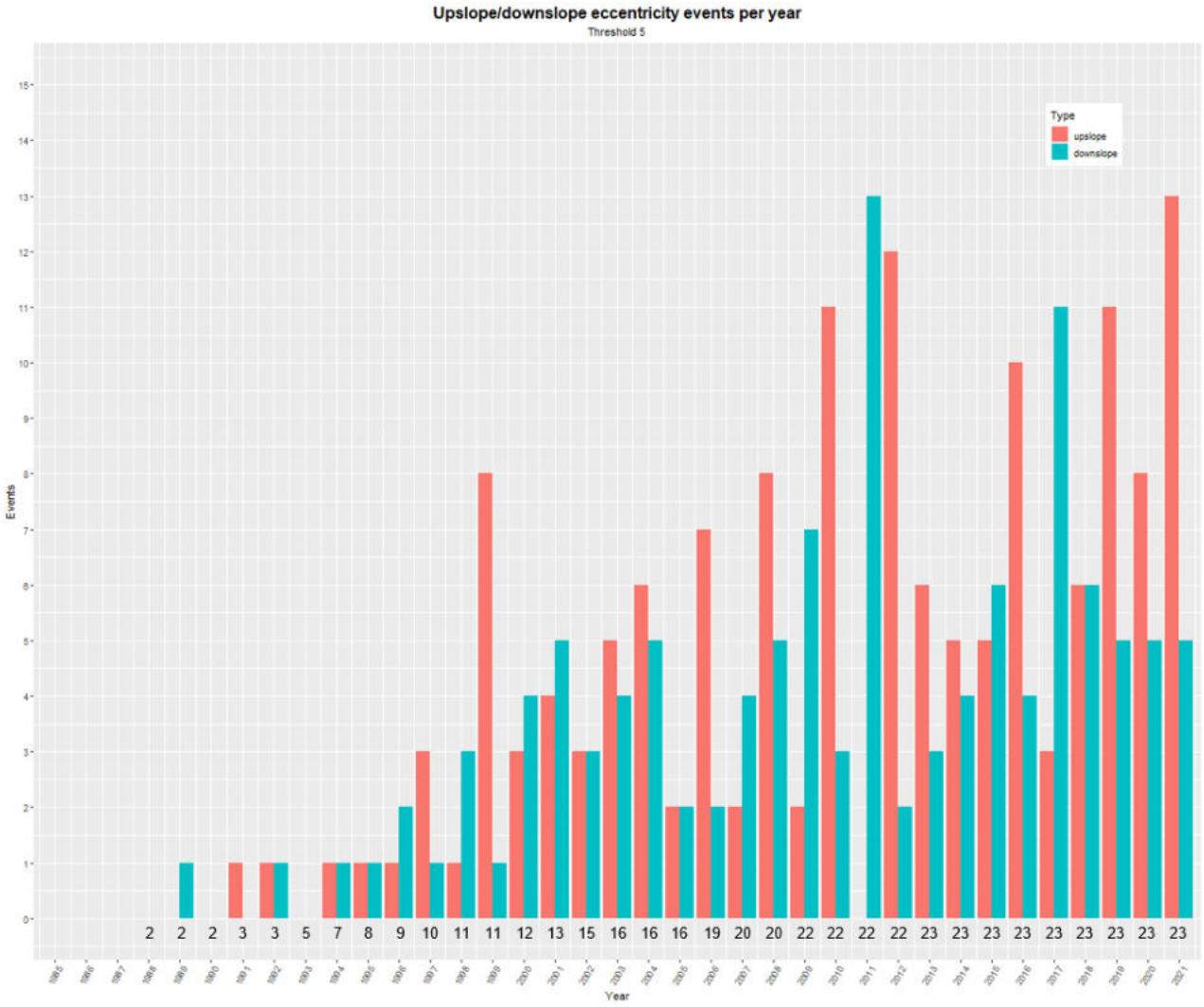

Figure 25: Eccentricity events in sampled birch trees exceeding threshold 5.

As shown in table 3, threshold 5 is much smaller than the previous ones. Therefore, more events can be seen in figure 25. The oldest dated event is from 1989. Trends are similar to the already presented plots above. Many upslope and downslope events are visible in the end of the x-axis. Prominent upslope years can be detected during 1999, 2006, 2008, 2010, 2012, 2016 and 2019-2021. Especially the years 1999, 2010, 2012 and 2021 are standing out. Prominent downslope events can be observed in 1998, 2007, 2009, 2011 and 2017 with the most striking in 2011 and 2017.

Differently than in the previous three figures, the following three figures depict also events exceeding the same thresholds. However, here the eccentricity values were averaged and plots with the mean eccentricity per year were drawn. See also chapter 4.6 for a more detailed explanation. On the x-axis, the years are depicted, on the y-axis, *vEix* is shown. If the curve passes the positive/negative line then an event leading to more eccentricity is assumed. Similar as above, the oldest dated birch stems from 1986 and altogether 23 trees were used for the analysis. Below each graph, just above the x-axis, the total number of trees per year is depicted.

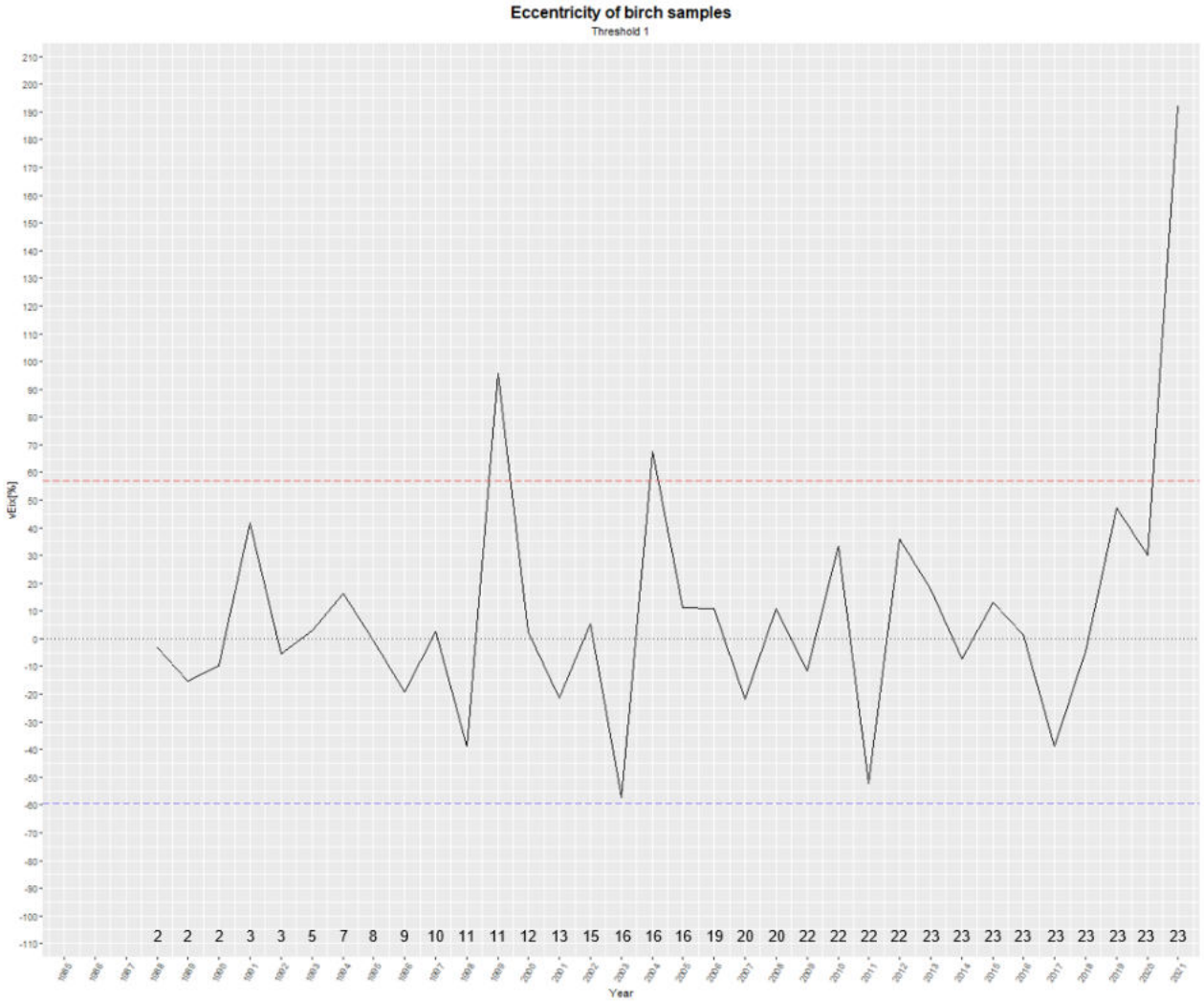

Figure 26: Eccentricity events of birch trees being marked by horizontal lines. Here, threshold 1 is used.

Events exceeding threshold 1 are shown in figure 26. Upslope eccentricity events exceeding threshold 1 can be observed in years 1999, 2004 as well as 2021. Downslope eccentricity events cannot be distinguished in any of the years, due to none of the events exceeding the threshold.

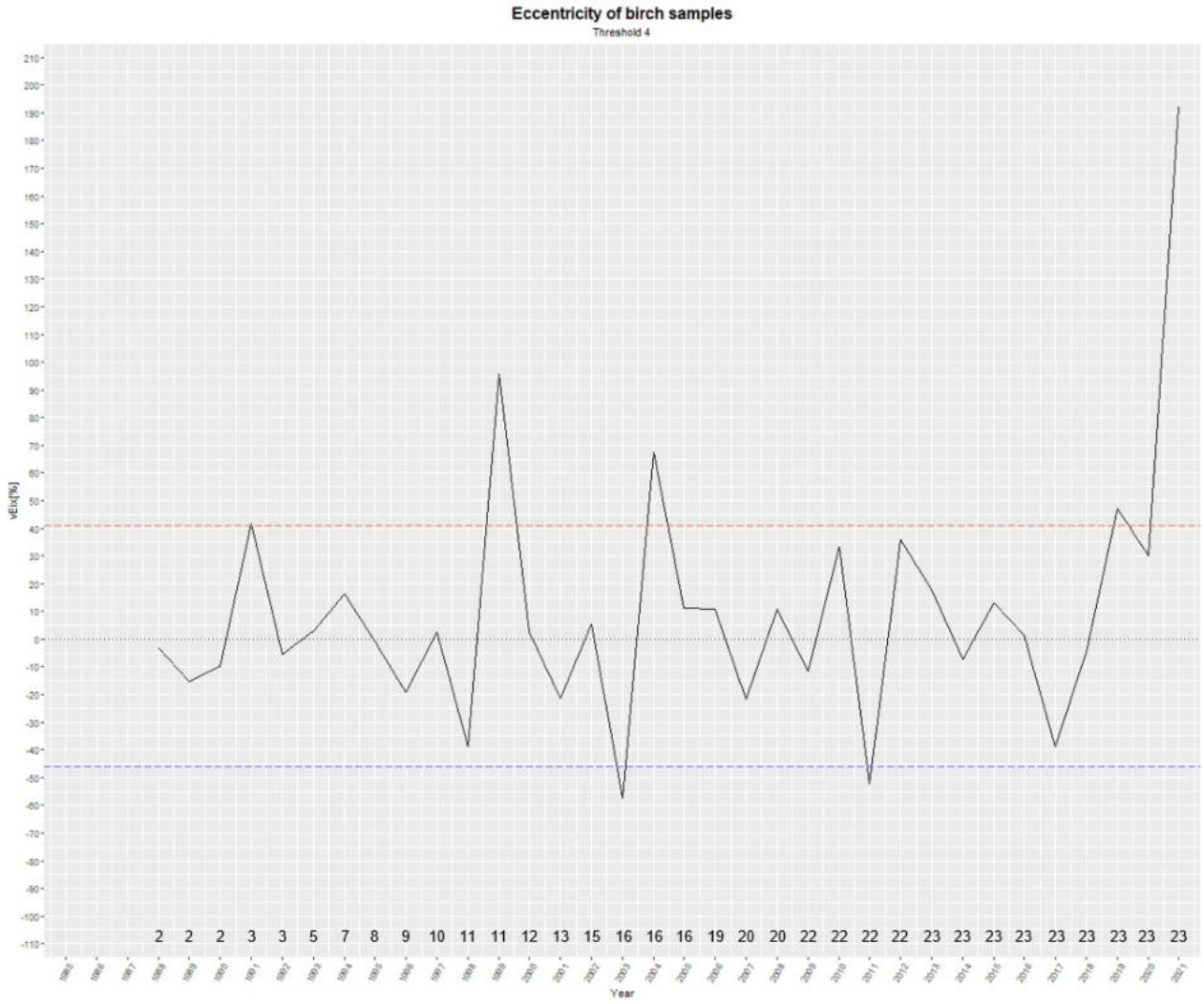

Figure 27: Eccentricity events of birch trees being marked by horizontal lines. Here, threshold 4 is used.

Events exceeding threshold 4 are shown in figure 27. Similarly as in the previous figure, upslope events can be distinguished in years 1991, 1999, 2004, 2019 and 2021. Downslope events can be observed in 2003 and 2011.

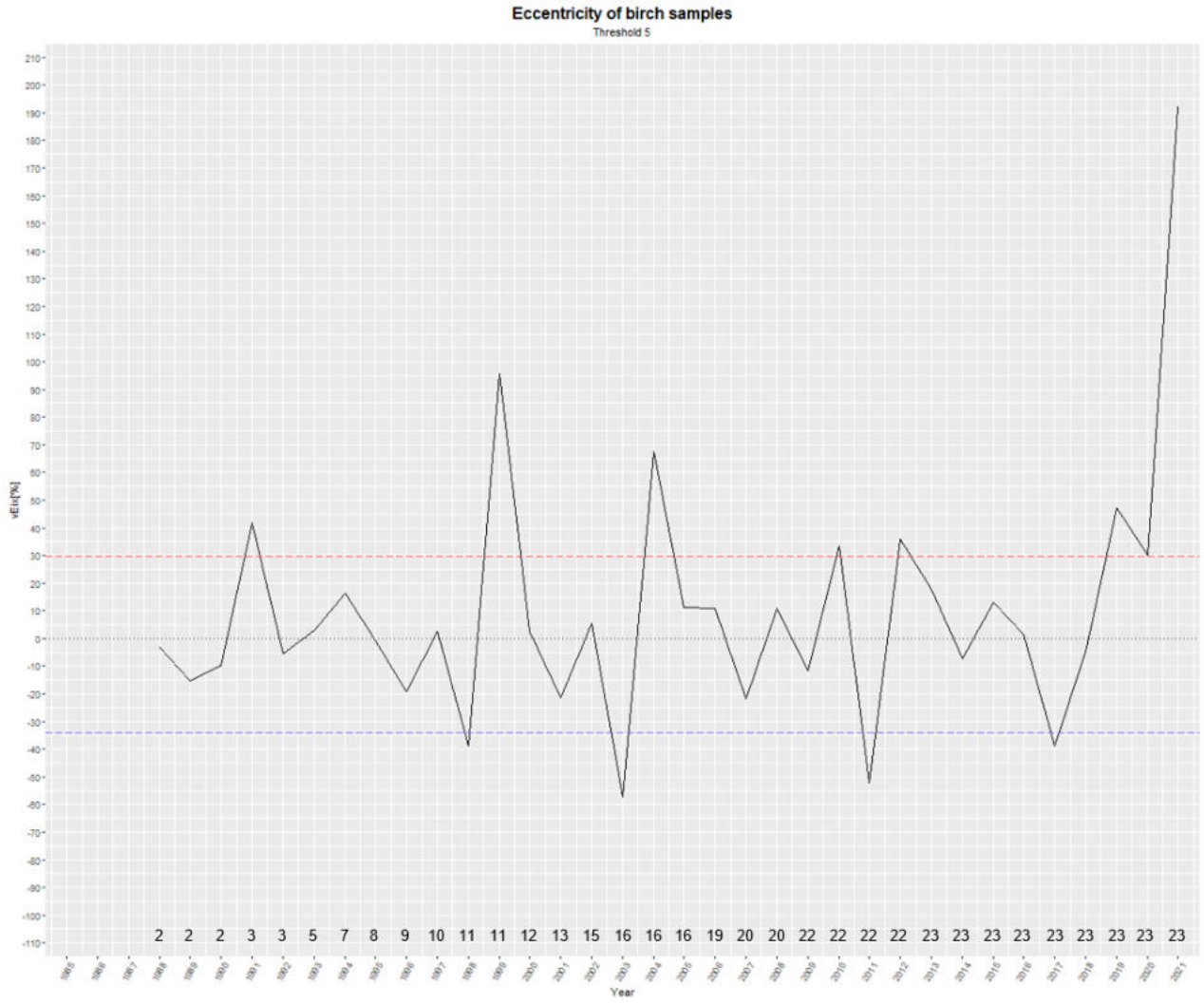

Figure 28: Eccentricity events of birch trees being marked by horizontal lines. Here, threshold 5 is used.

In figure 28, eccentricity events exceeding threshold 5 are presented. Upslope event years can be marked in 1991, 1999, 2004, 2010, 2012 and 2019-2021. Downslope events can be seen in 1998, 2003, 2011 and 2017.

Even though the oldest birch tree used for the analysis and the last six depicted plots is dated back to 1986, the eccentricity index starts at 1988. This is due to one tree, dated back to 1986, not having the same amount of tree-rings, respectively lacking the resolution due to damage whilst coring.

5.2 Eccentricity and compression wood area analysis

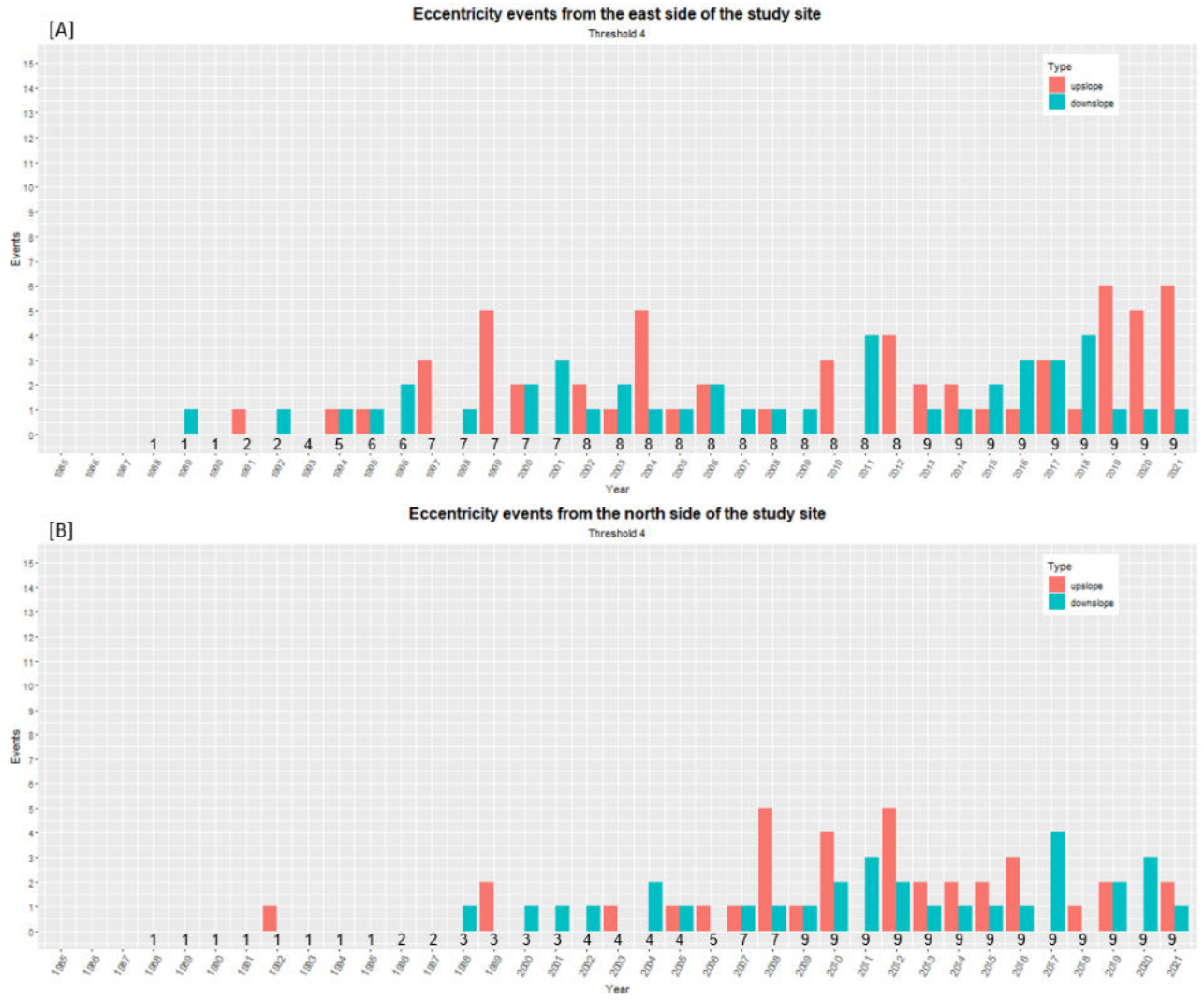

Figure 29: Birch upslope and downslope events at sites eastern and northern to the slope. Groups were selected with eight to the east respectively nine birch trees north of the study site.

Figure 29 depicts upslope/downslope eccentricity events containing nine trees each. One group on the east [A] side of the study site and the other group northerly [B] of the study site. The graph is the same as in figure 35, also using threshold 4. As can be seen, generally more events are visible in [A] than in [B]. Furthermore, upslope events on the eastern side are prominent in years 1997, 1999, 2004, 2010, 2012 as well as from 2019 to 2021. Downslope events are visible in years 1996, 2001, 2011 and 2018. Upslope events on the northern side of the study site can be assessed in years 2008, 2010 and 2012 with prominent downslope events in 2011, 2017 and 2020.

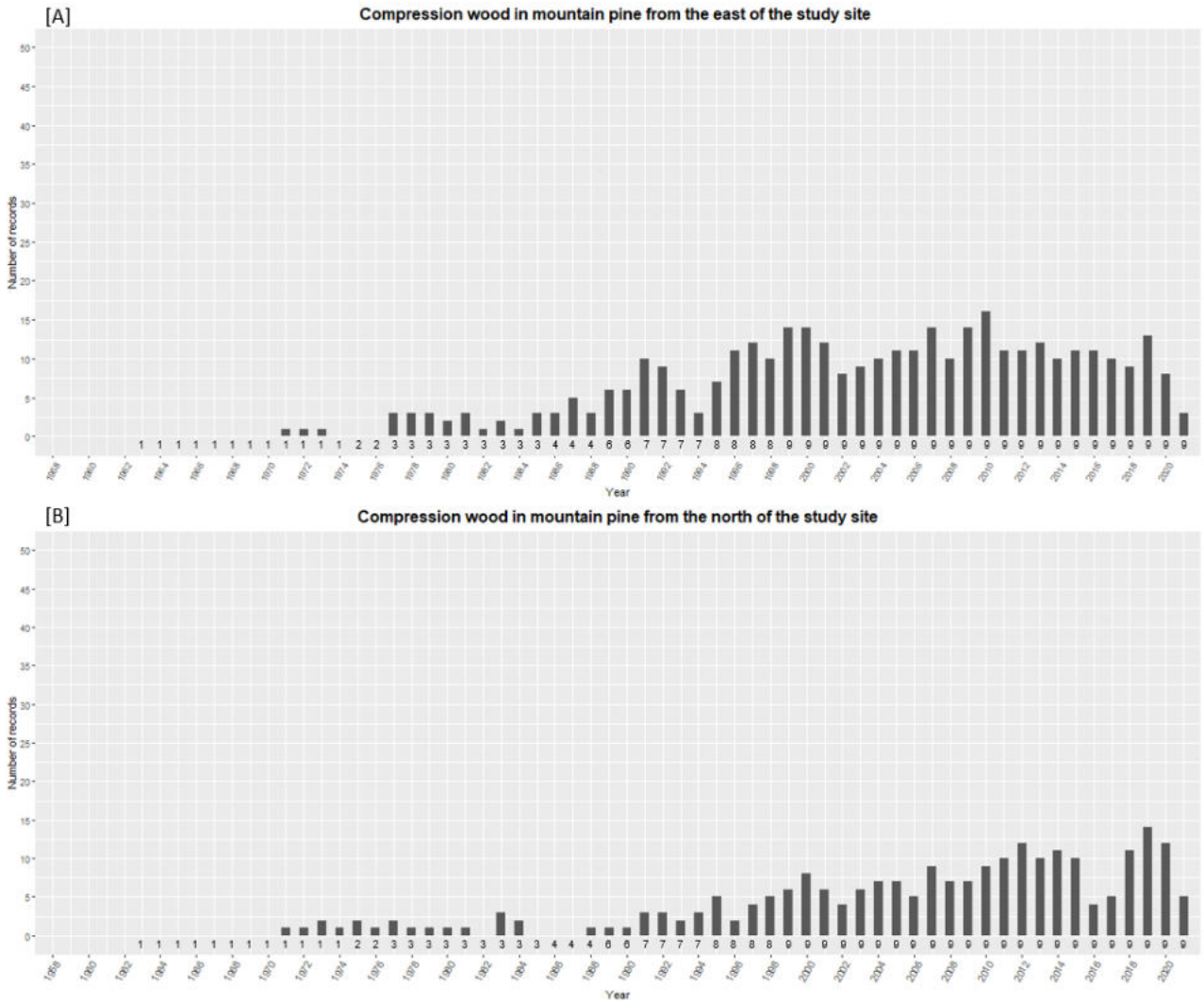

Figure 30: Compression wood in mountain pine sampled in two groups. Groups were selected with nine and eight trees per group. The first group is clustered to the east, while the second is located to the north of the study site.

Similarly as in the previous one, figure 30 depicts two groups, containing nine and eight trees. The first one is located on the eastern [A] side of the study site, whereas the lower one is made up of trees northerly [B] of the study site. Compression wood was dated visually, same as in figure 32. Generally, more events are recorded in [A] than in [B]. Prominent compression wood years in the group on the eastern side are 1991, 1997, 1999-2000, 2007, 2010 and 2019. In the northern group, compression wood can predominantly be found in years 2000, 2007, 2012, 2014 and 2019-2020.

5.3 Birch injuries

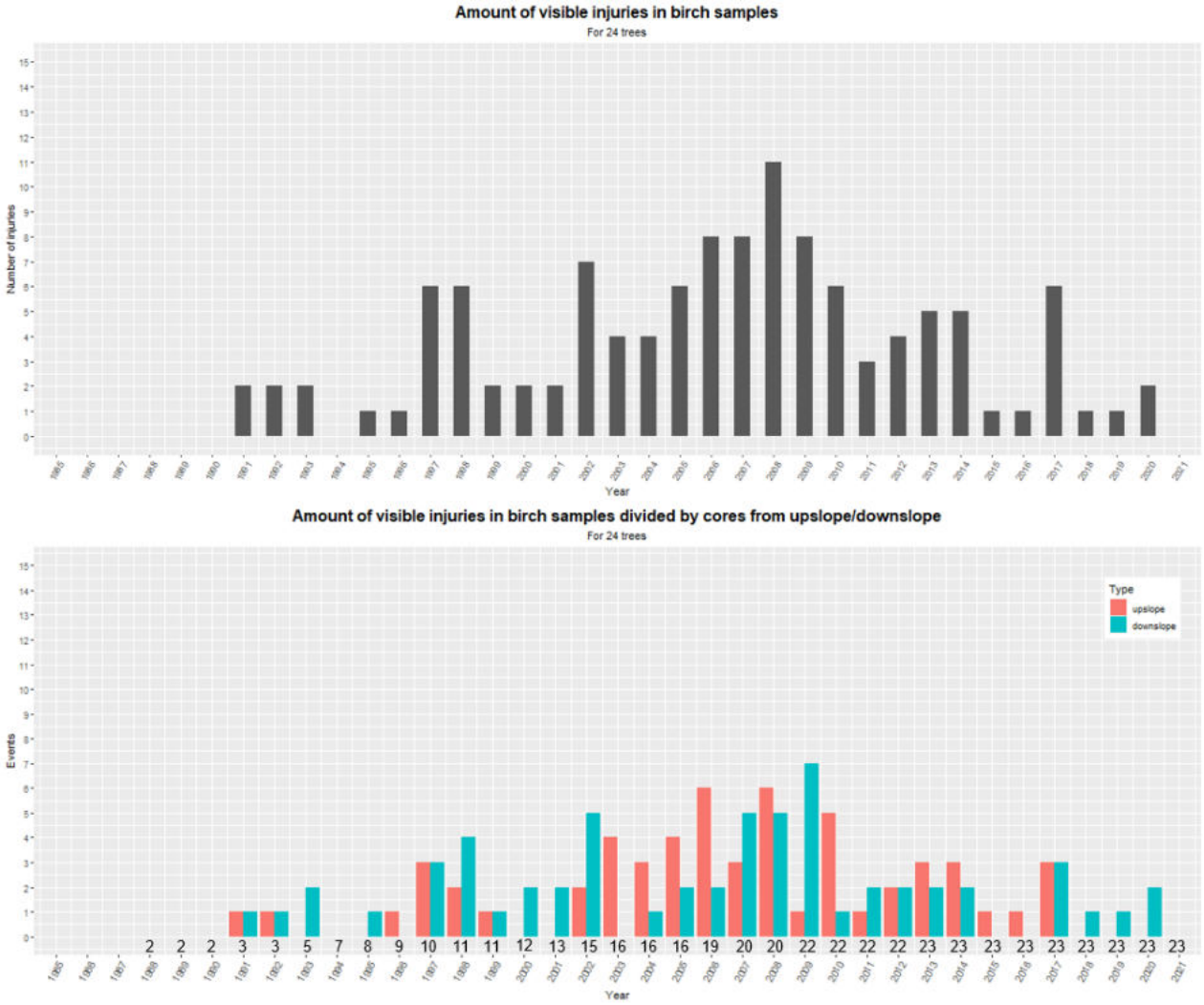

Figure 31: Injuries in birch trees, depicting total amount of injuries above and separated in upslope and downslope below.

In figure 31, injuries in birch trees have been dated visually and plotted accordingly in the upper part of the figure. In the lower part, the injuries are split between upslope and downslope, meaning that the injury was either found in an upslope core or downslope respectively. Firstly, peering at the upper graph reveals that more injuries happened during the years 2005-2010, as well as some in 1997-1998 and one peak in 2017. If compared to the upslope/downslope graph below, injuries during the years 2005-2010 seemed to have happened predominantly affecting the upslope side, shifting to the downslope side from 2007-2009. Other peaks in 1997-1998 seem to be balanced equally, similarly with the peak in 2017. In total, 24 trees were sampled and used for the analysis.

5.4 Pine compression wood

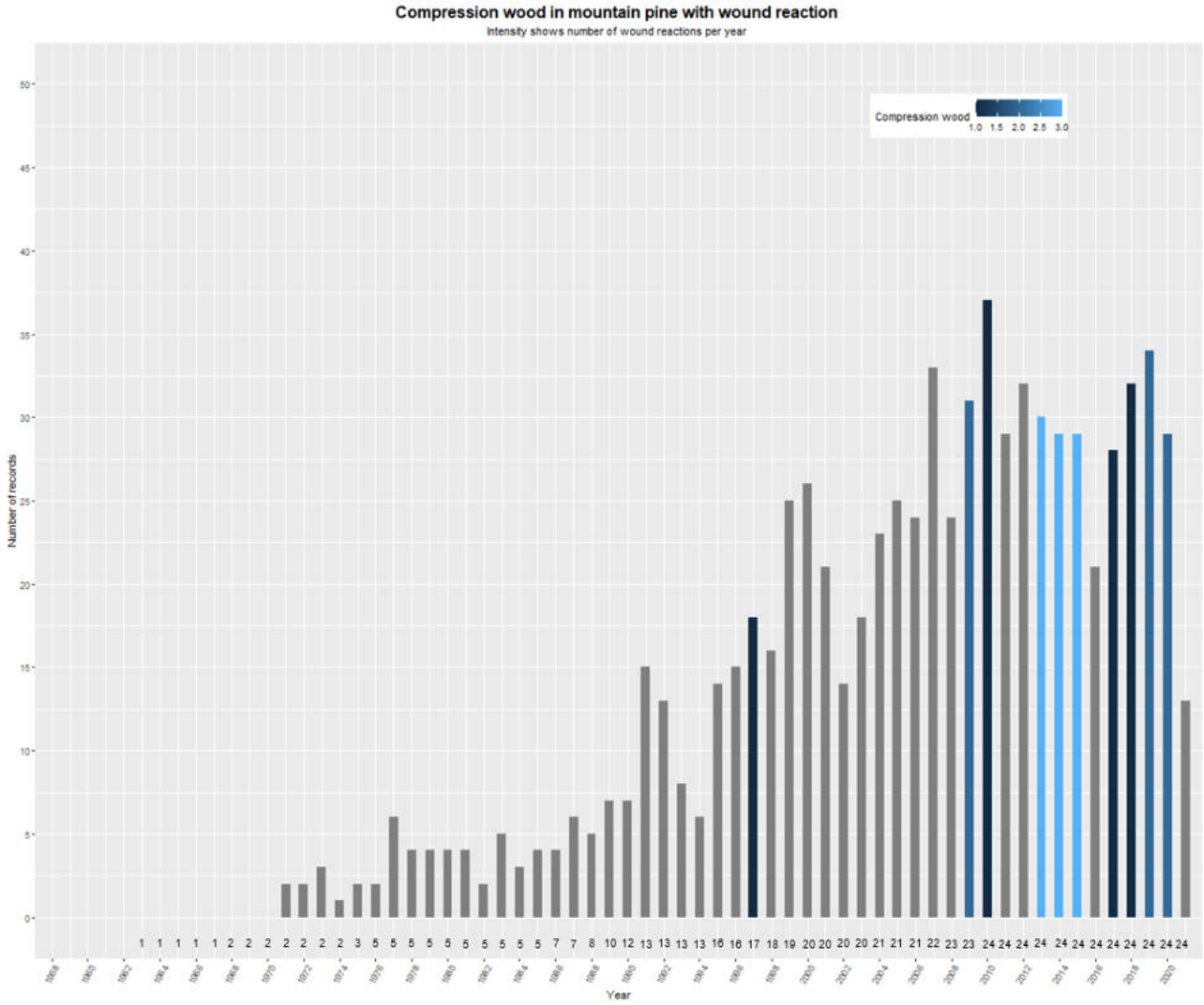

Figure 32: Compression wood observations made in mountain pine samples. In blue the amount of wound reactions in absolute numbers in samples.

In figure 32, compression wood found in mountain pine samples is depicted. The compression wood, often exhibited for many years in a row, was dated visually. Just above the x-axis the total number of trees per year is depicted. In total, 24 pine trees were used. Moreover, the number or records incorporate all found compression wood in all samples. This means that even if a tree had several samples taken they were counted as well and added to the total number in that year. The oldest tree is dated back to 1963, with only very few trees being older than 1980. As for example, 13 trees were used in 1994, compared to only 5 trees in 1985. In 1999, 19 trees were used, whereas from 2010 on, all of the 24 were used for the analysis of compression wood. Therefore, observing a trend in the data is rather hard, due to the uneven number of trees and observations of compression wood. The first observation of compression wood is from 1971, before that, zero observations were made. If glanced at in detail, many compression wood peaks can be made out, starting in 1991-1992 on to 1997, 1999-2000,

2007, 2009-2015 and 2017-2020. Also, in blue, wound reactions, due to a disturbance or injury, are depicted. These wound reactions were found in the tree-rings and refer to the injury happening in the year before. Such observations have been made in 1997 with only one event. Furthermore, in 2009-2010 as well as relatively many events in 2013-2015 as well as in single events in 2017-2018 and some in 2019-2020.

5.5 Thin sections

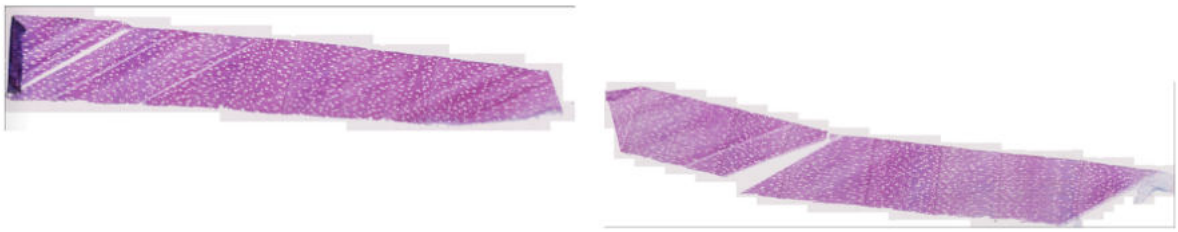

Figure 33: Two thin sections of birch sampled from upslope.

Thin sections were prepared in order to prove tension wood in birch samples. The generating of thin sections is explained in detail in chapter 5.5. It was intended to produce thin sections of each birch tree, however this was stopped due to the samples not exhibiting tension wood. Several trees were used to make thin sections, not as planned, none of them showed any tension wood in the year rings. Also, both upslope and downslope cores were made use of. In figure 33, a thin section of one birch tree is displayed, tension wood would be visible in tightly packed blue cells. Injuries in tree rings, such as in figure 34, were easy to spot.

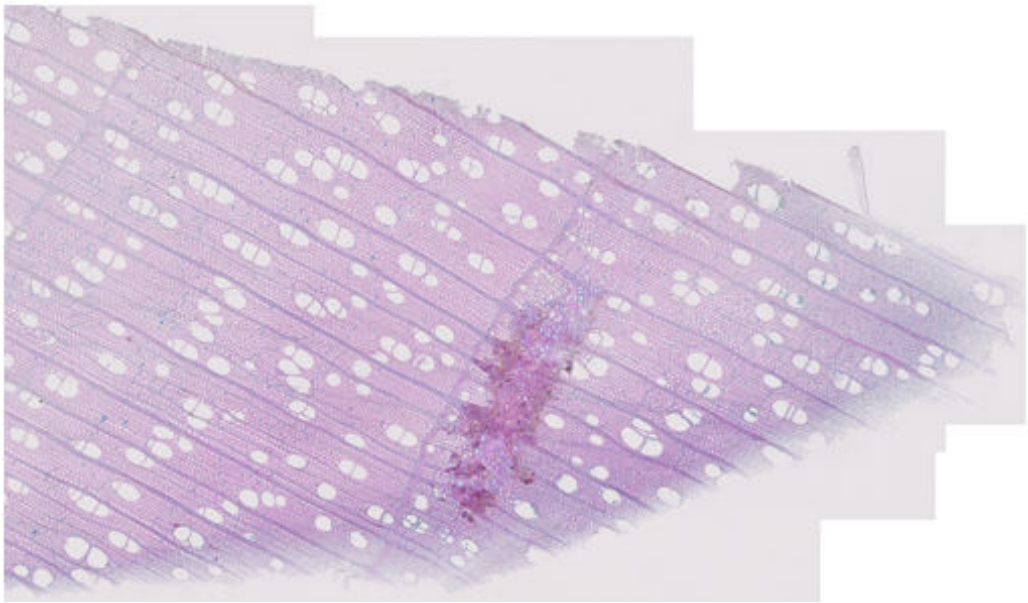

Figure 34: Injury visible in thin section from birch sampled from downslope. Depicted is a injury happening in the end of the growing season.

6 Discussion

In this section the results of this thesis are discussed. This part is structured into an interpretation part of the main findings of snow avalanche events and in answering the research objectives.

6.1 Summary of eccentricity events

Firstly, the main results of the eccentricity events of figures 23 to 25 are summed up. Overall, eccentricity of trees surpassed the threshold dramatically in years 1999, 2006, 2008, 2010, 2012, 2016, 2019 and 2021. Next to these events, smaller peaks do exist, exhibiting big to large events. However, here the focus was on the biggest ones. Main results of the eccentricity plots exceeding the thresholds in figures 26 to 28 are summed up as follows: In general, main upslope events, presumably by snow avalanches, can be distinguished in years 1999, 2004, 2008, 2010, 2019 and 2021. Years 1991, 2010 and 2012 displayed eccentricity in a somewhat reduced type. Concerning 1991, even though events were especially registered in the latter three figures, it was generally lacking a clear signal in the first three figures. This is due to the fact that only three trees were old enough to show signs of eccentricity in that year, therefore 1991 is discarded. Concerning 2008 and 2010, many events were noticed in nearly all of the figures, therefore they are added to the main events as well. Additionally, main downslope events, presumably not influenced by snow avalanches, occurred in years 2003, 2011 and 2017.

6.2 Threshold selection

Six thresholds were calculated in this thesis. After reviewing the different effects each threshold had on the determination of events, only one threshold was selected. The threshold, which was calculated from the birch reference, determines from which point on a tree is showing eccentric growth (see table 3 in the *methods* section). Hence the normal value of eccentric growth for a tree tilted upslope and downslope in the study site is above or below the specified thresholds. The decision to use on threshold is based on the fact, that a reasonable amount o events should be identified. Thresholds with too few and too many events, such as threshold 3 and 6 are excluded. Threshold 1 and 2 are rather similar, with the exception that threshold 2 depicts more downslope events. However, since the values are high, only few eccentricity events are identified and thus, both are discarded. Eventually, the choice falls between threshold 4 and 5. Since threshold 5 is quite similar to threshold 6 and possibly also shows too many events, threshold 4 is selected as the final one. More on the calculation of this in a later section.

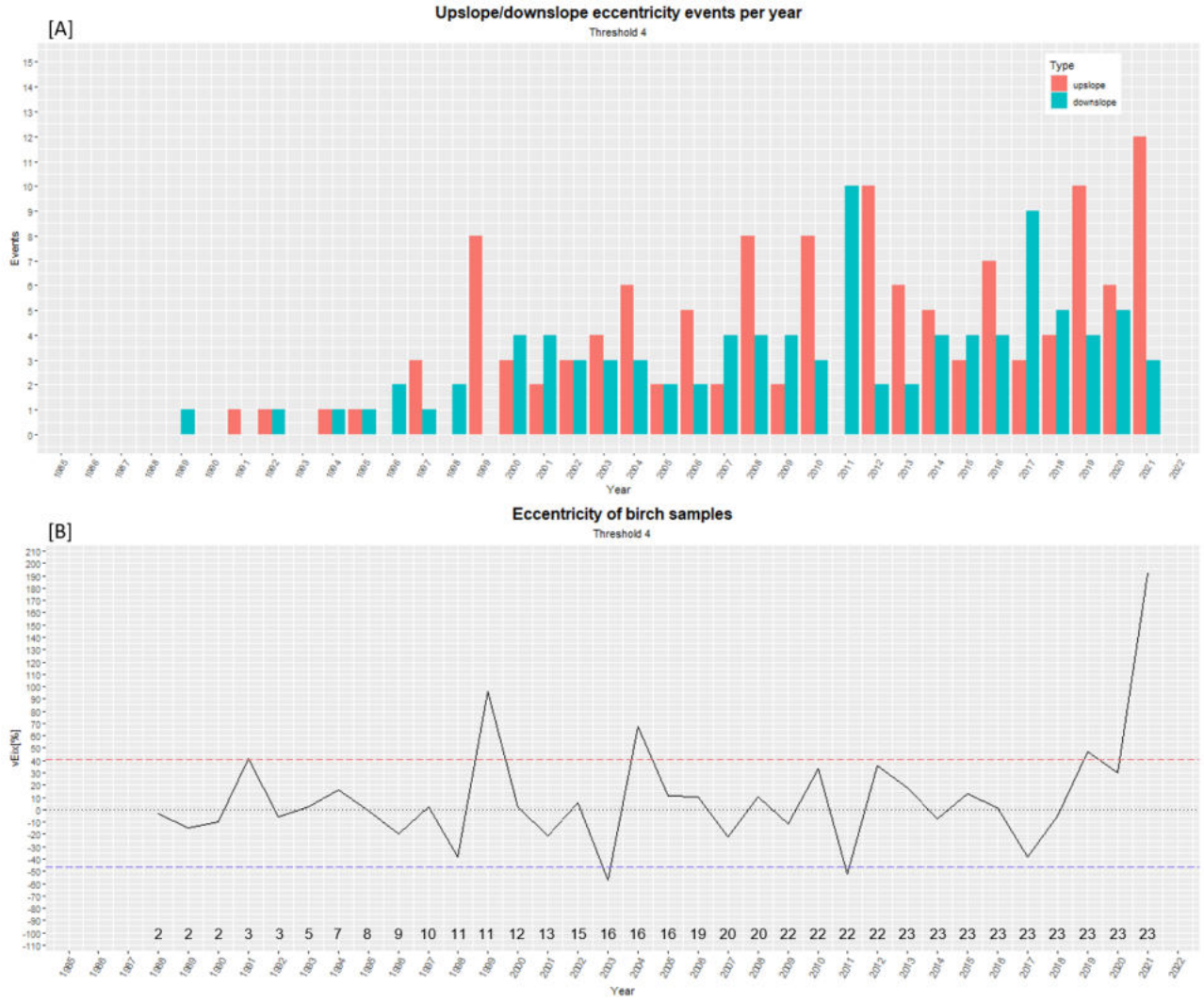

Figure 35: Eccentricity events determined using threshold 4. Under the lower figure, the number of trees per year is shown.

In figure 35, the events determined by threshold 4 are shown again. For a better visualisation and comparison, they are shown on top of each other (for more details see chapter 5). Both figures are using the same threshold and do exhibit similar events, with the upper figure being more distinct on when events have happened. As a result, upslope eccentricity events, likely induced through snow avalanches, are determined in years 1999, 2004, 2010, 2012, 2019 and 2021. Whereas downslope eccentricity events can be distinguished in 2011 and 2017. Predominantly, upslope events prevail, which means that radii of stems were larger on the upper side. Events are likely to be led back to snow avalanches, due to the reason that the study site is mainly affected by snow avalanches. The next section will discuss the interpretation of events in detail.

6.3 Interpretation of eccentricity events

The upper part [A] of figure 35 applies the threshold to each *vEix* value of every tree for each year, whereas the lower part [B] takes the mean of *vEix* and simply applies a horizontal threshold line, in order to distinguish events. This leads to the question, which one of the methods is more sensible to use? By simply glancing at the figures, it is visible that both show quite similar peaks, however, there is some mismatch during the years 2003 and during 2006-2009. Especially 2003 seems to be quite different, with lots of upslope events displayed in [A] and the opposite shown in [B]. For this part, and in general, figures applying the threshold to every value of each year of each tree are more sensible and to be preferred [A]. This is due to the *vEix* value being more true to the actual eccentricity in the trees than the averaged value over all years. Nevertheless, displaying the averaged *vEix* values [B] does help to visually determine eccentricity. The setting of a threshold is a crucial task. Often also a rather general view, since the mean value of the reference trees might not reflect well to the sensitivity of an individual tree. For example, during the the prominent avalanche year 1999 (Eidg. Institut für Schnee- und Lawinenforschung, 2000), not all trees reached the threshold of 40.98, even if neighboring trees did so. In addition, for the whole series the *vEix* values at times were only slightly above/below the threshold, therefore, simply adjusting the threshold in order to find a reasonable amount of events might not lead to the desired result (Burkhalter et al., 2019). Same goes for part [B] of figure 35, where years 1991 and 2019 are only slightly above the threshold. As a possible solution, fuzzy thresholds could be introduced. Such fuzzy sets are stemming from statistics. Instead of focusing on if a value is above or below a threshold, they introduce a gradual crossing from non-member to member (Nachtegael et al., 2003). This could possibly be applied to include eccentricity values very close to the threshold. It should be noted that even if no event has been noted by the eccentricity analysis, it does not mean that no snow avalanche possibly occurred.

Considering [A], if a large difference between upslope and downslope bars exist, one can assume that in most trees, the upslope tree rings were definitely larger. Thus, an event or process must have happened. Since birch trees exhibit tension wood, an abrupt increase in growth on the upper side as well as less growth on the opposite side mark an eccentricity event. In this case, the first year of the rapid increase is taken as an event year, since the tree might also produce tension wood years after the event occurred due to ongoing skewing (Burkhalter et al., 2019; Casteller et al., 2007; Decaulne et al., 2011). This also explains the selection of the events which are classified as snow avalanches. Years 2005-2007 and 2013-2015 show exactly this sort of behaviour, signs of a tree trying to regain its vertical position. Usually for snow avalanche reconstructions, evidence for snow avalanche damage should be visible in 10-40% of individual trees for a given year (Luckman, 2010). If compared to figure 35 and use the middle trigger point of 30% of trees, all the set event years can be confirmed. However, this use of an index is usually not in use in combination with eccentricity and snow avalanche studies. In addition, a higher sample depth would be highly advisable, in order to identify events (Butler et al., 2008; Corona et al., 2012; Decaulne et al., 2011). With regard to building a snow avalanche chronology of disturbed and damaged trees, a minimum of ten trees is suggested, where more is better, of course (Butler et al., 2008).

Another question revolves around in what way a downslope eccentricity event can be explained, in trees, that naturally form tension wood on the upslope side. One explanation of high downslope eccentricities, such as in 2011 and 2017, could be to balance growth towards vertical growth, after effects such as snow masses, wind or own weight changed the positioning of a tree (Wistuba et al., 2013). Possible are also sudden changes through mass-movements in the ground, changing the cardinal point towards the crown points (Wistuba et al., 2012). Eccentricity may also not occur immediately, but rather years after an event has happened (Šilhán et al., 2015). Such could have been the case, since the area around the Göscheneralp received above normal amounts of precipitation in 2010. Possibly leading to landsliding in the following year (Zbinden, 2010). Landslides often do not match years with lots of precipitation (Wistuba et al., 2012). During the year 2011, the northern side of the Alps received disproportionately low amounts of precipitation (MeteoSchweiz, 2011). Interestingly, the same applies to the rather precipitation-rich year 2016, which reported mud- and landslides, as well as the rather below average rainfall during the summer of 2017 (MeteoSchweiz, 2016, 2017). Another approach to explain the year 2011 is discussed in the subsequent section.

Eccentricity in trees may not only be traced back to a geomorphic event. Influences such as unequal development of roots and crown as well as moisture deficits can also lead to eccentric growth (Casteller et al., 2007). Furthermore, trees are also influenced by general snow pressure and creeping snow, leading to eccentric growth (Schweingruber, 1996). Another problem is, that it is not possible to clearly reconstruct the intensity of a snow avalanche with reaction wood, especially when multiple snow avalanches happen during a year (Casteller et al., 2007). A major shortcoming is that the reconstruction of a snow avalanche may be erroneous, since the event might have happened after the growing season, only being displayed in annual rings during the following year. Reasoning in that regard can however rarely be found in the literature. The differentiation if a snow avalanche or a debris flow has happened, can be made through the positioning of injuries and callus tissue during a year (Kogelnig-Mayer et al., 2011). Snow avalanche reconstructions, by dating scars, have been done successfully (Veblen et al., 1994). Therefore, for this thesis, coupling the differentiation between snow avalanche and landslide would have been useful, and should be included in a similar thesis.

6.3.1 Thin sections

Thin sections of several trees were produced, as described in the *results*. Proving tension wood in trees, by identifying the anatomical properties, therefore, would have been helpful. Unfortunately, none of them showed any tension wood. This then answers the second subquestion of the second research objective. Thin sections would have been assistant to increase the accuracy of dating of events (Burkhalter et al., 2019). A thin section, which exhibits tension wood, is depicted in the *appendix*.

6.4 Comparison to snow avalanche chronology

In this section, the set events will be compared to the existing snow avalanche chronology from the region as well as discussing reports from the hydrological calendar years. This section also aims to answer the first research objective, stated in the beginning in chapter 1.1.

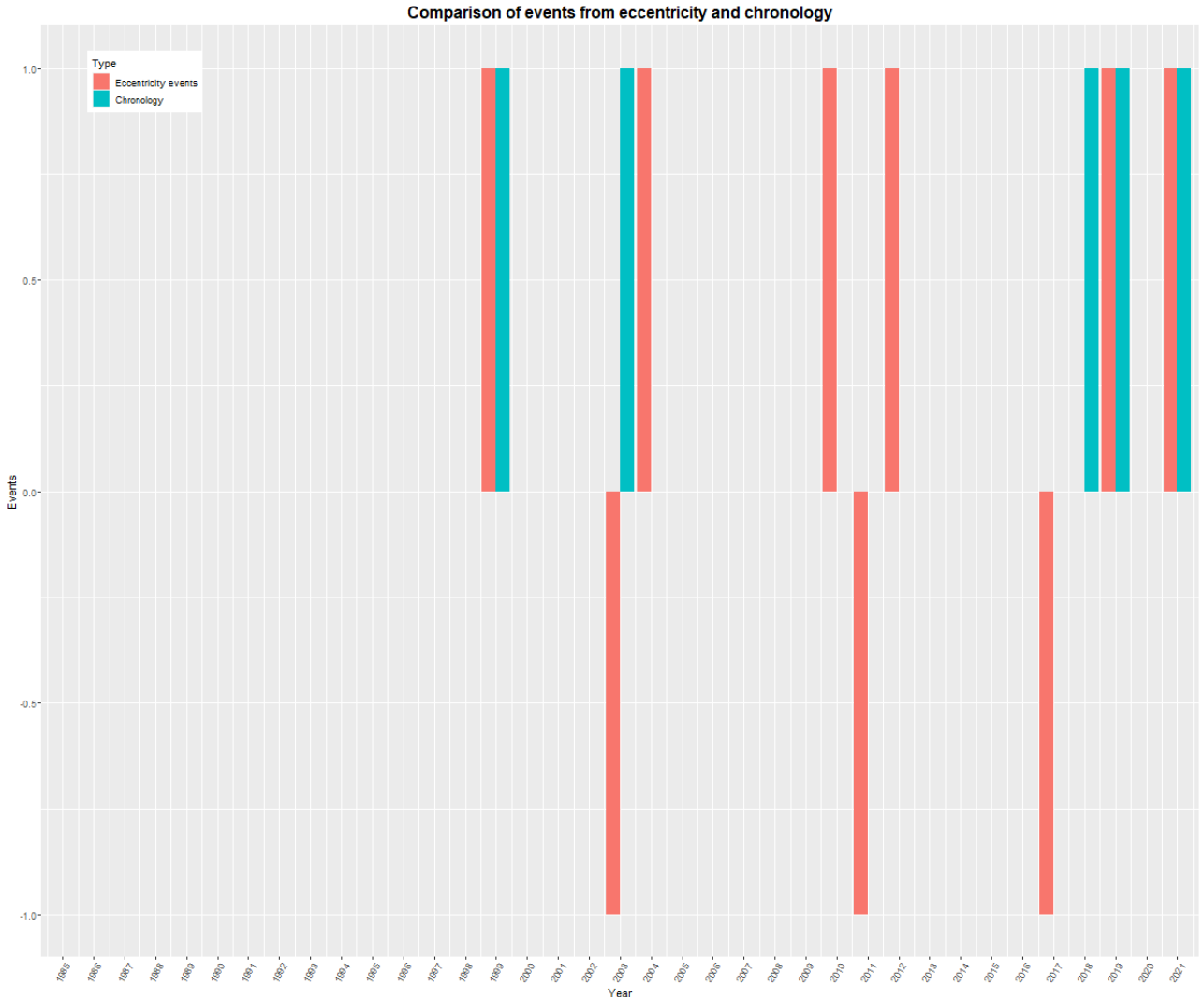

Figure 36: Events determined by eccentricity depicted alongside events determined from existing snow avalanche chronology at the study site. In red are the eccentricity events previously defined and in blue from the official chronology.

Data on the snow avalanche records at the study site has been gathered from the canton Uri as well as from the SLF and presented in detail in table 1 in the section on the *study site*. In figure 36, the eccentricity events determined by the chosen threshold have been depicted alongside the official chronology. Upslope eccentricity events, interpreted as snow avalanche events, have been given the value 1. Downslope events are marked by the value -1. Events from the chronology received the value 1. If both bars appear right next to each other, snow avalanche events have been noted in both

datasets. This is the case in years 1999, 2019 and 2021. These are also the years in which upslope eccentricity was most distinct. Moreover, 1999 was a year with enormous amounts of snow, leading to multiple snow avalanches in the whole of Switzerland and Europe (Eidg. Institut für Schnee- und Lawinenforschung, 2000). Next to this, 2019 and 2021 both are exceptional snow avalanche years, as can be inferred from reports by the SLF (Zweifel et al., 2021, 2019). A large snow avalanche at the study site can also be seen in the *theory* section in figure 7. Years 2010 and 2012 have been noted in the eccentricity analysis but no records exist in the snow avalanche chronology. This due to not many records for the study site existing. Also, there is sometimes a bias to list only major events, which caused considerable damage to infrastructure (Bollschweiler et al., 2011; Corona et al., 2012). Even though the precipitation amounts for the winter 2009/2010 were on average, the snow cover composition was unfavourable which led to many snow avalanches during early and late winter (Etter et al., 2012). The year 2012, in contrast, was very rich in amounts of snow, which led to many snow avalanches damaging forest and infrastructure (Techel et al., 2013). As can be seen in figure 36, year 2004 was also determined to show snow avalanches due to eccentricity but is lacking an entry in the chronology. The peak of the upslope eccentricity (figure 35) is slimmer than in other years. The SLF report of 2004 describes a rather mixed snow and temperature situation. In the Gotthard region, many wet snow avalanches took place during May as well as larger dry snow avalanches during January (Wiesinger et al., 2005). At this point, it has to be cautiously considered if the year 2004 can be counted as an event year. The year 2003 is interesting due to the fact that the chronology shows a snow avalanche event and the index a downslope eccentricity event. This may very well be, since a powder avalanche occurred opposite of the study site and presumably affected trees on the downslope side. Therefore, as a compensation, the birch trees were forming tension wood on the side of the disturbance. However, this should be taken with a grain of salt, since only part [B] of figure 35 shows a downslope event. There is also a record for the year 2018, with no event from the index. This can be explained since the snow avalanche occurred at Hutzgen, which lies to the west of the study site. It was included due to possibly affecting the study site, however, it seems to be spatially far enough apart from the study site. Year 2011 in the eccentricity analysis shows a downslope event with no record in the chronology. Hydrologically, the year 2011 was extraordinarily dry. Almost no precipitation occurred in spring and with an excessive amount in late July (BAFU, 2015). Therefore, landslides or slope movement could have been the cause of the downslope eccentricity, since a sudden change of rainfall might have promoted such a process (Handwerger et al., 2019).

As a result of the comparison, the snow avalanche reconstructions done with help of the eccentricity index can be compared relatively well to the existing snow avalanche chronology. Furthermore, also smaller events, not noted in the chronology, seem to appear. This may very well be, since only the largest events tend to be noted in records (Corona et al., 2012).

6.5 Spatial eccentricity and compression wood analysis

Here, it is discussed if the snow avalanches might have been spatially divided at the study site. Also, discussing the last of the research objectives.

Firstly, the eastern side of the study site is analysed, represented in [A] in figures 29 and 30. In general, more events are visible in [A] than in [B], which could imply more disturbances occurred east than north of the study site. Furthermore, upslope events seem to coincide in years 1997, 1999, 2010 and 2019 with compression wood formation. This could presumably be led back to snow avalanche events during these years, as partly discussed in the previous section. As already described, accurately determining compression wood in mountain pine samples is difficult, since it is exhibited nearly in all years. Years 2004 and 2012 bare quite clear signs in the eccentricity plot but remain vague in the compression wood. In 2004, many upslope events were noted at the eastern group whereas in the northern group only some downslope events are marked. Therefore, a snow avalanche possibly occurred on the eastern side, sparing the northern group, but affecting some trees in that way that they were tilted into direction of the slope. Year 2021 is quite clear in the eccentricity plots but shows few signs of compression wood formation. This is similar to figure 32, also not showing any particular signs. This might be due to differences in the vegetation period of the mountain pine. It may also be possible, that it is difficult to detect when the ring has not completely been formed. Downslope eccentricity events cannot be conclusively determined with compression wood formation.

To sum up, snow avalanche events probably occurred at the eastern side of the study site in years 1997, 1999, 2004, 2010, 2012 and 2019. These are events which can be shown both in eccentricity and compression wood. Other years are difficult to determine, using the same approach. Also, landslide or slope movements probably affected trees in the eastern group in 2011 and 2018. With the former more probable, as already discussed. More events were noticed on the eastern side, which leads to the conclusion that the eastern side is more frequently affected by snow avalanches. In a picture, taken in summer 2021, it is quite evident that a snow avalanche strongly affected the trees on the eastern side of the study site (figure 46 in the *appendix*).

Following, the analysis of the group on the northern side of the study site, as shown in [B] in both figures. Years in which both figures show possible events are 1999, 2012 and possibly also 2008. Again, compression wood analysis offers a very unclear signal, exacerbated by less signals and less trees used. Eccentricity shows clear upslope signals in 2010, but not so clear compression wood findings. Therefore, if both eastern and northern groups are regarded, a snow avalanche could have impacted both groups in 2010. Snow avalanches were probably only influencing the northern group in 2008 and 2010, not affecting the eastern part of the study site. Though compression wood in 1999 in the northern group is not as succinct, it surely must have impacted both groups. This due to it being such a heavy snow avalanche year. A downslope event in 2011 was very similar to the other group, leading to the conclusion that the whole study site might have been affected by landslides. Further, another slope movement event might have only affected the northern group, with no clear signs in the eastern group. Interestingly, 2020 was noted with as a strong downslope event with considerable compression wood.

In the eastern group this is inverted. Hence, a landsliding event could have impacted only the northern group again.

To sum up, snow avalanches probably occurred at the northern side of the study site in years 1999, 2010, 2012 and 2008. Prominent downslope event presumably influenced by slope movements can be inferred in years 2011, 2017 and 2020.

6.6 Compression wood in pine and comparison to snow avalanche events

Most snow avalanche reconstruction have been using reaction wood as a means to reconstruct events (Butler et al., 1985; Carrara, 1979; Corona et al., 2010; Garavaglia et al., 2011) as well as coupled with eccentricity (Casteller et al., 2007). Here, compression wood findings (see figure 32) are compared to eccentricity analyses from the previous sections. It can be expected that, when there was a snow avalanche event, compression wood should coincide with that.

Events from the eccentricity index match compression wood of pine in 1999, 2010, 2012 and 2019. The year 2004 is difficult to determine, since a definite peak of compression wood is missing. Similarly in 2021, where it is possible that the compression wood has not yet been formed at the time of sampling. In the beginning of the timeline, not many trees were used, possibly adding to the uncertain determination of compression wood trends. Wound reactions can also be found at times and always refer to an incident happening in the year before. Of course, a wound reaction could also have happened in the same year. These injuries correspond well to events of 2012 as well as 2019. Overall, a pattern is hard to identify, since these reactions can also stem from rockfall in summer and general snow cover from winter. Injuries were often on small branches of a tree. Furthermore, 1997 seemed to produce some compression wood also correlating to a smaller upslope event which was however not noted in the discussion. What can be noted is that the high numbers of compression wood sightings between 2004-2020 are confusing. This can either be due to more trees being used as well as to the mountain pine not being the optimal species to reconstruct snow avalanches from. This would also explain the general lack of studies involving mountain pine for snow avalanche reconstructions. Compression wood determination was difficult to identify visually, because the mountain pine exhibits this type of reaction wood very frequently. This due to the fact that the tree grows creeping along the floor and often in snow avalanche paths (Alexandrov et al., 2019). Mountain pines rarely grow straight and are also bent by smaller slides and general snow cover (Bebi et al., 2009). As a result, the species are quite flexible and often produce reaction wood.

Adding to this, the samples from the mountain pine were overall very young, which is not beneficial for dating disturbances (Tonelli et al., 2020). Often, the first 10-20 years of records from a tree are not taken into account, which would have been detrimental to this analysis. It is also difficult to determine older events, since traces thereof might have been swept off by more recent snow avalanches (Luckman, 2010). More often, snow avalanche reconstructions are done with spruce or fir species, exhibiting a clearer compression wood signal (Corona et al., 2010). Only rarely, studies are conducted with mountain pine (Muntán et al., 2009). From the results of this thesis, it is suggested to use an

alternative species than the mountain pine, in order to accurately date a snow avalanche event. To answer the third research question, compression wood was able to be compared to the largest events of the eccentricity index. However, it failed to conclusively be used as a means to confirm the eccentricity events. The initial dating and and cross-dating was challenging, owing to the unclear year ring borders and uncertain beginning of compression wood formation. Additionally, compression wood findings show a pattern rather than than the exact findings. Upslope, downslope and at times several samples of a tree were used to display compression wood.

6.7 Birch injuries and comparison to snow avalanche events

Birch injuries (see figure 31) were dated visually from the high-resolution photographs done with Skippy. As has been done in studies to reconstruct debris flows by dating injuries in birch trees (Arbellay et al., 2010), it was expected that injuries might coincide with the determined events by snow avalanches. However, none of the dated injuries match the dated events. For example, 1999 is an obvious snow avalanche year, which should have left scars or other marks as a result. Contrasting to this, almost no injuries were noted as can be seen in figure 31. This could be since the snow avalanche either fully destroyed certain trees or simply bent them without any visible injuries at the stem. One exception thereof is the year 2008, which does show some injuries. The eccentricity index (figure 35) does show some events in [A] but not in [B], also there is no record from the official chronology. Further, mostly smaller injuries were noted. Overall, injuries seem to have happened rather through rockfall than by snow avalanches. This due to the injuries appearing primarily often at the end of a ring. This shows that the injury must have happened during the end of the growing season in summer and, therefore, more likely by rockfall. This leads to the conclusion that dating snow avalanches through injuries is not possible at the study site and the eccentricity index offers a better method. This then answers the second subquestion of the third research objective. This may also confirm that the study site is strongly influenced through rockfalls in the summer - as can be seen by the many boulders and rocks in the field (see figure 45 in *appendix*).

Figure 37: Injuries in three birch samples. Here, year 1998 is shown with the injury appearing close to the border of the year ring. Pictures were taken in CooRecorder.

It is possible that scars or injuries are just not visible in the cores taken, due to the injury happening at a different side of the tree (Arbellay et al., 2010). Moreover, smaller and younger trees might simply

bend with an incoming snow avalanche and, therefore, not show any visual signs of disturbance such as an injury (Bebi et al., 2009). This is likely since the trees in this study are extremely young, the oldest birch is dated to 1986.

6.8 Calculation of thresholds

The threshold certainly represents one of the most important aspects of an eccentricity analysis. Determining how high or low the threshold is, decides where event years took place and serves as backbone of a study revolving around reconstructing landslides, mud flows or snow avalanches. Contrasting to this, the calculation or determination of thresholds are rarely discussed in detail. For the most part, the standard deviation is added to the mean of the positive/negative eccentricity, which results in one value each (Malik et al., 2016; Šilhán, 2019; Wistuba et al., 2012; Wistuba et al., 2013; Wistuba et al., 2018). Other studies define a threshold without much discussion, sometimes also using a different eccentricity analysis (Casteller et al., 2008; Casteller et al., 2007; Garavaglia et al., 2011). Also, most often in the literature, reference trees were cored parallel to the slope inclination, same goes for the disturbed trees. Here in this thesis, reference cores were extracted perpendicular to the slope. In an optimal setting, reference trees are selected growing straight and undisturbed. Since the study site is located in a mountainous and narrow valley, finding such a reference is indeed very hard to impossible. Therefore, taking cores parallel to the slope for the reference might have been more useful in order to distinguish events and build a better threshold. However, landslides and slope movement cannot be fully accounted for when distinguishing events. This due to it being very hard to determine in a natural environment which is influenced by many processes at the same time.

Focusing again on the calculation. Threshold 4 was calculated by taking the median instead of the mean. Under normal circumstances, the mean is more accurate in portraying the actual value for a group of samples. I argue that since the reference is not located in a totally undisturbed spot, the median is a more sensitive method, due to it being less susceptible to outliers. For example, mean reference eccentricity for year 1994 is *51.52* whereas the median is *-1.28*. This discrepancy is due to two trees, used to calculate the mean, exhibit extraordinary high values. This is enough to obscure the threshold and render it quite much higher in total. The calculation by mean for threshold 3 results in *-50.31* and *65.33* whereas the calculation, with the same base values, for threshold 4 lie at *-46.22* and *40.98*. Consequently, the median may give more applicable results, especially in high disturbance environments such as at the study site. In environments where reference trees are growing undisturbed and outliers in eccentricity are very seldom to be found, the mean may be the preferable method.

As already mentioned, most of the literature is calculating threshold values by taking the mean and the standard deviation. In almost all cases however, the precise calculation of the threshold is missing. It is not entirely clear if the positive/negative values are calculated by taking the mean and standard deviation for all the positive and negative values. Or if instead the values per year are averaged and then the positive/negative values are taken together with the standard deviation as final values. Since the threshold is very essential to every eccentricity analysis, it would be very helpful to reveal the exact

calculation of positive and negative threshold values. As has been done in this thesis (see eccentricity calculation in chapter 4.6), the mean (or median) of every year was taken and if it was positive, added to the positive value column. Same goes for the negative values. This produced two columns, where the individual eccentric value of a tree perished in light of one averaged value. This might be reasonable in samples which are very uniform but seems artificial if the stand is even only slightly dissimilar.

Together with the discussion on the other thresholds, this subsection answers the second research objective. Threshold 4 seems as a reasonable choice to use to determine event years of snow avalanches. A different threshold may still show the largest events, but might however also produce too many event years. In the end, the threshold selection is relatively arbitrary and may also be approximated to the desired effect, which is not very objective in itself. A small change in calculation can result in rather different values, as for threshold 1 & 2 and threshold 3 & 4. Besides, determining what counts as an event is up to the research question or the aim of a study. Showing too many events might be desirable, if the goal was to assess as many disturbances to trees as possible, but less so to date large-scale events.

For that reason, it would be desirable if a set mechanism to determine the threshold accurately could be developed. This seems to be a research gap which could be explored.

7 Conclusion

This thesis aimed to reconstruct snow avalanches via an eccentricity analysis and reaction wood dating. For that, two rarely used tree species, namely the silver birch and the mountain pine, were utilized. For the birch an eccentricity analysis was used, whereas compression wood was examined for the mountain pine. Along with, injuries on trees and thin sections of birch were consulted in order to provide additional evidence of disturbance events.

In conclusion, years 1999, 2008, 2010, 2012, 2019 and 2021 are regarded as years in which snow avalanches occurred. This was decided after evaluating the different sections of the discussion. In addition, the whole study site presumably was affected by landslides or other slope movements in years 2011 and 2017. However, this cannot be stated absolutely and should be studied in detail. Regarding research objective [1], *Do the dated snow avalanche events coincide with an already existing chronology?* Years coincide with the chronology in 1999, 2019 and 2021. A major limitation of snow avalanche chronologies is, to only include major events. Therefore, not all of the dated events being congruent to the existing chronology is possible.

Continuing with research objective [2], *Can an accurate eccentricity threshold be chosen?* A totally accurate threshold is probably impossible to obtain, each tree reacts individually to its environment. Generalizing a value however, serves as a good approximation. Threshold 4, which was chosen in this thesis, provided a reasonable amount of events. Differences of calculated thresholds are shown in the *results* and *discussion*, answering the subquestion to [2]. To sum up, a threshold can be accurate, if it fulfills the goals of a study and is interpreted cautiously. Since the clear calculation of a thresholds is often missing in the literature, it would be favourable to produce a common method for the calculation of eccentricity thresholds.

Research objective [3], *Can the dated eccentricity events in birch be compared to compression wood formation in pine?* Most studies use compression wood in order to date snow avalanches, sometimes also combined with eccentricity. Years from the eccentricity index pair well with compression wood findings in mountain pine in 1999, 2010, 2012, 2019. However, the findings suggest using a different tree species than mountain pine in order to distinguish events. The mountain pine is showing compression wood frequently which blurs a clear picture. Therefore, it is possible in part to compare eccentricity events to compression wood findings in mountain pine, but should be regarded in a critical light. As to subquestion [3a], thin sections of birch were unable to verify tension wood. In this case, discs might have been preferable. Furthermore, injuries in the birch trees could not be attributed to years of snow avalanche events, answering subquestion [3b]. A study examining injuries more closely might however bring different results, since a clear differentiation between rockfall and snow avalanche is possible.

As to the last research objective [4], *Can the dated snow avalanche reconstruction be spatially defined?* Snow avalanches presumably occurred on the whole study site in 1999 and 2010. The northern group must have experienced a large event in 2008, which was not recorded in the eastern group. In turn,

snow avalanche have affected only the eastern side in years 1997, 2004, 2019 and 2021. Hence, snow avalanches at the study site can be spatially divided to year and location.

So far, not many snow avalanches have been reconstructed via an eccentricity analysis, especially not with the mentioned tree species. This thesis has shown that it is potentially possible, but should be regarded critically. Compression wood dating with mountain pine needs to be examined either in detail or another tree species should be consulted. Dating of tree-rings was tough in mountain pine, due to the missing of clear year-ring borders. This could have yielded wrong dating and also a wrong finding of compression wood. Furthermore, the visual dating of compression wood and injuries is a rather vague concept and should possibly be done anatomically. Overall, the eccentricity analysis yielded a fair result, though the calculation of a threshold poses a major limitation. Another major constraint is that the disturbance event, as analyzed by the eccentricity index, might have happened in the year before but only shows in the following growing season. More research in the area of threshold calculation could clarify and set the standard for a supported and well-founded threshold. Also, rendering a high accuracy for the dating of disturbance events.

8 Bibliography

References

Alexandrov, A., Wühlisch, G. von, Vendramin, G. (2019). "EUFORGEN Technical Guide- lines for genetic conservation and use for mountain pine (Pinus mugo)." October, p. 32611.

Arbellay, E., Stoffel, M., Bollschweiler, M. (2010). "Dendrogeomorphic reconstruction of past debris-flow activity using injured broad-leaved trees". *Earth Surface Processes and Landforms* 35.4, pp. 399–406. ISSN: 01979337. DOI: 10.1002/esp.1934.

BAFU (2015). *Hydrologisches Jahrbuch der Schweiz 2011*. Tech. rep. Bern: Bundesamt für Umwelt, p. 629.

Bätz, N., Colombini, P., Cherubini, P., Lane, S. N. (2016). "Groundwater controls on biogeomorphic succession and river channel morphodynamics". *Journal of Geophysical Research: Earth Surface* 121.10, pp. 1763–1785. ISSN: 21699003. DOI: 10.1002/2016JF004009. URL: http://doi.wiley.com/10.1002/2016JF004009.

Bebi, P., Kulakowski, D., Rixen, C. (2009). "Snow avalanche disturbances in forest ecosystems-State of research and implications for management". *Forest Ecology and Management* 257.9, pp. 1883–1892. ISSN: 03781127. DOI: 10.1016/j.foreco.2009.01.050.

Beck, P., Caudullo, G., Rigo, D. de, Tinner, W. (2016). "Betula pendula, Betula pubescens and other birches in Europe: distributon, habitat, usage and threats." *European Atlas of Forest Tree Species*, pp. 70–73.

Bernasconi, S. M., Bauder, A., Bourdon, B., Brunner, I., Bünemann, E., Chris, I., Derungs, N., Edwards, P., Farinotti, D., Frey, B., Frossard, E., Furrer, G., Gierga, M., Göransson, H., Gülland, K., Hagedorn, F., Hajdas, I., Hindshaw, R., Ivy-Ochs, S., Jansa, J., Jonas, T., Kiczka, M., Kretzschmar, R., Lemarchand, E., Luster, J., Magnusson, J., Mitchell, E. A., Venterink, H. O., Plötze, M., Reynolds, B., Smittenberg, R. H., Stähli, M., Tamburini, F., Tipper, E. T., Wacker, L., Welc, M., Wiederhold, J. G., Zeyer, J., Zimmermann, S., Zumsteg, A. (2011). "Chemical and Biological Gradients along the Damma Glacier Soil Chronosequence, Switzerland". *Vadose Zone Journal* 10.3, pp. 867–883. ISSN: 1539-1663. DOI: 10.2136/vzj2010.0129.

Bollschweiler, M., Stoffel, M., Schläppy, R. (2011). "Debris-Flood Reconstruction In A Pre-Alpine Catchment In Switzerland Based On Tree-Ring Records Of Coniferous And Broadleaved Trees". *Geografiska Annaler, Series A: Physical Geography* 93.1, pp. 1–15. ISSN: 04353676. DOI: 10.1111/j.1468-0459.2011.00001.x.

Braam, R. R., Weiss, E. E., Burrough, P. A. (1987). "Dendrogeomorphological analysis of mass movement a technical note on the research method". *Catena* 14.6, pp. 585–589. ISSN: 03418162. DOI: 10.1016/0341-8162(87)90008-7.

Brang, P., Schnenberger, W., Ott, E., Gardner, B. (2008). "Forests as Protection from Natural Hazards". *The Forests Handbook, Volume 2*. Oxford, UK: Blackwell Science Ltd, pp. 53–81. DOI: 10.1002/9780470757079.ch3. URL: https://onlinelibrary.wiley.com/doi/10.1002/9780470757079.ch3.

Bräuning, A., De Ridder, M., Zafirov, N., García-González, I., Dimitrov, D. P., Gärtner, H. (2016). "Tree-ring features: Indicators of extreme event impacts". *IAWA Journal* 37.2, pp. 206–231. ISSN: 22941932. DOI: 10.1163/22941932-20160131.

Bühlmann, T., Hiltbrunner, E., Körner, C. (2014). "Alnus viridis expansion contributes to excess reactive nitrogen release, reduces biodiversity and constrains forest succession in the Alps". *Alpine Botany* 124.2, pp. 187–191. ISSN: 1664221X. DOI: 10.1007/s00035-014-0134-y.

Burkhalter, P., Egli, M., Gärtner, H. (2019). "Reconstruction and actual trends of landslide activities in Bruust-Haltiwald, Horw, canton of Lucerne, Switzerland". *Geographica Helvetica* 74.1, pp. 93–103. ISSN: 21948798. DOI: 10.5194/gh-74-93-2019.

Burrows, C., Burrows, V. (1976). *Procedures for the study of snow avalanche chronology using growth layers of woody plant*. Tech. rep. Boulder, CO: Institute of Arctic and Alpine Research.

Butler, D. R., Sawyer, C. F. (2008). "Dendrogeomorphology and high-magnitude snow avalanches: A review and case study". *Natural Hazards and Earth System Science* 8.2, pp. 303–309. ISSN: 16849981. DOI: 10.5194/nhess-8-303-2008.

Butler, D. R., Malanson, G. P. (1985). "A History of High-Magnitude Snow Avalanches , Southern Glacier National Park , Montana , U . S . A ." *Mountain Research and Development* 5.2, pp. 175–182.

Butler, D. R. (1987). "Teaching General Principles and Applications of Dendrogeomorphology". *Journal of Geological Education* 35.2, pp. 64–70. ISSN: 0022-1368. DOI: 10.5408/0022-1368-35.2.64.

Carrara, P. E. (1979). "The determination of snow avalanche frequency through tree-ring analysis and historical records at Ophir, Colorado". *Bulletin of the Geological Society of America* 90.8, pp. 773–780. ISSN: 19432674. DOI: 10.1130/0016-7606(1979)90<773:TDOSAF>2.0.CO;2.

Carrer, M., Nola, P., Eduard, J. L., Motta, R., Urbinati, C. (2007). "Regional variability of climate-growth relationships in Pinus cembra high elevation forests in the Alps". *Journal of Ecology* 95.5, pp. 1072–1083. ISSN: 00220477. DOI: 10.1111/j.1365-2745.2007.01281.x.

Casteller, A., Christen, M., Villalba, R., Martínez, H., Stöckli, V., Leiva, J. C., Bartelt, P. (2008). "Validating numerical simulations of snow avalanches using dendrochronology: The Cerro Ventana event in Northern Patagonia, Argentina". *Natural Hazards and Earth System Science* 8.3, pp. 433–443. ISSN: 16849981. DOI: 10.5194/nhess-8-433-2008.

Casteller, A., Stöckli, V., Villalba, R., Mayer, A. C. (2007). "An evaluation of dendroecological indicators of snow avalanches in the Swiss Alps". *Arctic, Antarctic, and Alpine Research* 39.2, pp. 218–228. ISSN: 15230430. DOI: 10.1657/1523-0430(2007)39[218:AEODIO]2.0.CO;2.

Casteller, A., Villalba, R., Araneo, D., Stöckli, V. (2011). "Reconstructing temporal patterns of snow avalanches at Lago del Desierto,southern Patagonian Andes". *Cold Regions Science and Technology* 67.1-2, pp. 68–78. ISSN: 0165232X. DOI: 10.1016/j.coldregions.2011.02.001. URL: http://dx.doi.org/10.1016/j.coldregions.2011.02.001.

Cherubini, P. (2021). "Tree-ring dating of musical instruments". *Science* 373.6562, pp. 1434–1436. ISSN: 10959203. DOI: 10.1126/science.abj3823.

Corona, C., Lopez Saez, J., Stoffel, M., Bonnefoy, M., Richard, D., Astrade, L., Berger, F. (2012). "How much of the real avalanche activity can be captured with tree rings? An evaluation of classic dendrogeomorphic approaches and comparison with historical archives". *Cold Regions Science and Technology* 74-75, pp. 31–42. ISSN: 0165232X. DOI: 10.1016/j.coldregions.2012.01.003. URL: http://dx.doi.org/10.1016/j.coldregions.2012.01.003.

Corona, C., Rovéra, G., Lopez Saez, J., Stoffel, M., Perfettini, P. (2010). "Spatio-temporal reconstruction of snow avalanche activity using tree rings: Pierres Jean Jeanne avalanche talus, Massif de l'Oisans, France". *Catena* 83.2-3, pp. 107–118. ISSN: 03418162. DOI: 10.1016/j.catena.2010.08.004. URL: http://dx.doi.org/10.1016/j.catena.2010.08.004.

Coutand, C., Jeronimidis, G., Chanson, B., Loup, C. (2004). "Comparison of mechanical properties of tension and opposite wood in Populus". *Wood Science and Technology* 38.1, pp. 11–24. ISSN: 00437719. DOI: 10.1007/s00226-003-0194-4.

Decaulne, A., Eggertsson, O., Sæmundsson, P. (2011). "A first dendrogeomorphologic approach of snow avalanche magnitude-frequency in Northern Iceland". *Geomorphology* 167-168, pp. 35–44. ISSN: 0169555X. DOI: 10.1016/j.geomorph.2011.11.017. URL: http://dx.doi.org/10.1016/j.geomorph.2011.11.017.

Dube, S., Filion, L. (2004). "Tree-Ring Reconstruction of High-Magnitude Snow Avalanches in the". *Arctic, Antarctic, and Alpine Research* 36.4, pp. 555–564.

Dümig, A., Smittenberg, R., Kögel-Knabner, I. (2011). "Concurrent evolution of organic and mineral components during initial soil development after retreat of the Damma glacier, Switzerland". *Geoderma* 163.1-2, pp. 83–94. ISSN: 00167061. DOI: 10.1016/j.geoderma.2011.04.006. URL: http://dx.doi.org/10.1016/j.geoderma.2011.04.006.

Eidg. Institut für Schnee- und Lawinenforschung (2000). *Der Lawinenwinter 1999. Ereignisanalyse.* Eidg. Institut für Schnee- und Lawinenforschung, p. 588. ISBN: 3905620804.

Etter, H.-J., Stucki, T., Techel, F., Zweifel, B. (2012). *Schnee und Lawinen in den Schweizer Alpen. Hydrologisches Jahr 2009/2010.* Tech. rep., p. 78.

Fritts, H. (1976a). "Growth and Structure". *Tree Rings and Climate.* Chap. 2, pp. 55–117. DOI: 10.1016/b978-0-12-268450-0.50007-0.

— (1976b). "The Climate—Growth System". *Tree Rings and Climate.* Chap. 5, pp. 207–245. DOI: 10.1016/b978-0-12-268450-0.50010-0.

Garavaglia, V., Pelfini, M. (2011). "The role of border areas for dendrochronological investigations on catastrophic snow avalanches: A case study from the Italian Alps". *Catena* 87.2, pp. 209–215. ISSN: 03418162. DOI: 10.1016/j.catena.2011.06.006.

Gärtner, H., Schweingruber, F. (2013a). *Microscopic preparation techniques for plant stem analysis.* June, p. 78. ISBN: 9783941300767.

Gärtner, H., Heinrich, I. (2013b). "Dendrogeomorphology". *Encyclopedia of Quaternary Science: Second Edition* 2, pp. 91–103. DOI: 10.1016/B978-0-444-53643-3.00356-3.

Gärtner, H., Heinrich, I. (2009). "The Formation of Traumatic Rows of Resin Ducts in". *IAWA Journal* 30.2, pp. 199–215.

Gärtner, H., Nievergelt, D. (2010). "The core-microtome: A new tool for surface preparation on cores and time series analysis of varying cell parameters". *Dendrochronologia* 28.2, pp. 85–92. ISSN: 11257865. DOI: 10.1016/j.dendro.2009.09.002.

Germain, D., Hétu, B., Filion, L. (2010). "Tree-Ring Based Reconstruction of Past Snow Avalanche Events and Risk Assessment in Northern Gaspé Peninsula (Québec, Canada)". *Advances in Global Change Research* 41.March, pp. 51–73. ISSN: 22151621. DOI: 10.1007/978-90-481-8736-2{_}5.

Handwerger, A. L., Huang, M. H., Fielding, E. J., Booth, A. M., Bürgmann, R. (2019). "A shift from drought to extreme rainfall drives a stable landslide to catastrophic failure". *Scientific Reports* 9.1, pp. 1–12. ISSN: 20452322. DOI: 10.1038/s41598-018-38300-0.

Heinrich, I., Gärtner, H. (2008). "Variations in tension wood of two broad-leaved tree species in response to different mechanical treatments: Implications for dendrochronology and mass movement studies". *International Journal of Plant Sciences* 169.7, pp. 928–936. ISSN: 10585893. DOI: 10.1086/589695.

Kogelnig-Mayer, B., Stoffel, M., Schneuwly-Bollschweiler, M., Hübl, J., Rudolf-Miklau, F. (2011). "Possibilities and limitations of dendrogeomorphic time-series reconstructions on sites influenced by debris flows and frequent snow avalanche activity". *Arctic, Antarctic, and Alpine Research* 43.4, pp. 649–658. ISSN: 15230430. DOI: 10.1657/1938-4246-43.4.649.

Koprowski, M., Winchester, V., Zielski, A. (2010). "Tree reactions and dune movements: Slowinski National Park, Poland". *Catena* 81.1, pp. 55–65. ISSN: 03418162. DOI: 10.1016/j.catena.2010.01.004. URL: http://dx.doi.org/10.1016/j.catena.2010.01.004.

Krokene, P., Nagy, N. E. (2008). "Traumatic Resin Ducts and Polyphenolic Parenchyma Cells in Conifers". *Induced Plant Resistance to Herbivory*. Chap. 7, pp. 1–462. ISBN: 9781402081828. DOI: 10.1007/978-1-4020-8182-8.

Luckman, B. H. (2010). "Dendrogeomorphology and Snow Avalanche Research". *Advances in Global Change Research* 41, pp. 27–34. ISSN: 22151621. DOI: 10.1007/978-90-481-8736-2{_}2.

Malik, I., Wistuba, M., Migoń, P., Fajer, M. (2016). "Activity of slow-moving landslides recorded in eccentric tree rings of Norway spruce trees (Picea Abies Karst.) - An example from the kamienne MTS. (Sudetes MTS., Central Europe)". *Geochronometria* 43.1, pp. 24–37. ISSN: 18971695. DOI: 10.1515/geochr-2015-0028.

Maxwell, R. S., Larsson, L. A. (2021). "Measuring tree-ring widths using the CooRecorder software application". *Dendrochronologia* 67.December 2020, p. 125841. ISSN: 16120051. DOI: 10.1016/j.dendro.2021.125841. URL: https://doi.org/10.1016/j.dendro.2021.125841.

MeteoSchweiz (2011). *Klimabulletin Sommer 2011*. Tech. rep. Sommer, pp. 1–5.

— (2016). *Klimabulletin Sommer 2016*. Tech. rep. Sommer, pp. 1–5.

— (2017). *Klimabulletin Sommer 2017*. Tech. rep. Sommer, pp. 1–6.

Monteleone, I., Ferrazzini, D., Belletti, P. (2006). "Effectiveness of neutral RAPD markers to detect genetic divergence between the subspecies uncinata and mugo of Pinus mugo Turra". *Silva Fennica* 40.3, pp. 391–406. ISSN: 00375330. DOI: 10.14214/sf.476.

Muntán, E., García, C., Oller, P., Martí, G., García, A., Gutiérrez, E. (2009). "Reconstructing snow avalanches in the Southeastern Pyrenees". *Natural Hazards and Earth System Science* 9.5, pp. 1599–1612. ISSN: 16849981. DOI: 10.5194/nhess-9-1599-2009.

Nachtegael, M., Van der Weken, D., Van de Ville, D., Kerre, E. E. (2003). "Fuzzy Filters for Image Processing". *Fuzzy Thresholding and Histogram Analysis*, pp. 129–152.

Paul, F., Linsbauer, A., Haeberli, W. (2012). *Klimaänderung und Wasserkraft*. Tech. rep. August. Davos und Birmensdorf: Eidg. Forschungsanstalt für Wald, Schnee und Landschaft, p. 29.

Raden, M., Mattheis, A., Spiecker, H., Backofen, R., Kahle, H. P. (2020). "The potential of intra-annual density information for crossdating of short tree-ring series". *Dendrochronologia* 60.February, p. 125679. ISSN: 16120051. DOI: 10.1016/j.dendro.2020.125679. URL: https://doi.org/10.1016/j.dendro.2020.125679.

Rathgeber, C. B., Cuny, H. E., Fonti, P. (2016). "Biological basis of tree-ring formation: A crash course". *Frontiers in Plant Science* 7.MAY2016, pp. 1–7. ISSN: 1664462X. DOI: 10.3389/fpls.2016.00734.

Renner-Aschwanden, F. (2013). "Landschafts- und Waldgeschichte des Urserntals". *Historisches Neujahrsblatt / Historischer Verein Uri*.

Roloff, A., Weisgerber, H., Lang, U., Stimm, B. (2010). *Bäume Mitteleuropas*. Wiley -VCH Verlag GmbH & Co. KGaA.

RStudioTeam (2020). *RStudio: Integrated Development Environment for R*. Boston, MA. URL: http://www.rstudio.com/..

Schweingruber, F. H. (1988). *Tree Rings: Basics and Applications of Dendrochronology*. Kluwer Academic Publishers. ISBN: 9788578110796.

— (1996). *Tree Rings and Environment. Dendroecology*. Ed. by S. Swiss Federal Institute for Forest, L. Research. Birmensdorf, p. 609.

Schweizer, J. (2004). "Snow Avalanches". *Water Resources IMPACT* 6.1, pp. 12–18.

Šilhán, K. (2019). "Tree-ring eccentricity in the dendrogeomorphic analysis of landslides – A comparative study". *Catena* 174.November 2018, pp. 1–10. ISSN: 03418162. DOI: 10.1016/j.catena.2018.11.002.

Šilhán, K., Stoffel, M. (2015). "Impacts of age-dependent tree sensitivity and dating approaches on dendrogeomorphic time series of landslides". *Geomorphology* 236, pp. 34–43. ISSN: 0169555X. DOI: 10.1016/j.geomorph.2015.02.003.

Smith, K. T. (2008). "An organismal view of dendrochronology". *Dendrochronologia* 26.3, pp. 185–193. ISSN: 11257865. DOI: 10.1016/j.dendro.2008.06.002.

Speer, J. H. (2009). "Fundamentals of tree-ring research. James H. Speer." *Geoarchaeology* 26.3, pp. 453–455. ISSN: 1520-6548. DOI: 10.1002/gea.20357.

Spillmann, P., Labhart, T., Brücker, W., Renner, F., Gisler, C., Zgraggen, A. (2011). *Geologie des Kanton Uri*. Altdorf: Naturforschende Gesellschaft Uri (NGU). ISBN: 978-3-033-02916-3.

Stoffel, M., Bollschweiler, M. (2008). "Tree-ring analysis in natural hazards research - An overview". *Natural Hazards and Earth System Science* 8.2, pp. 187–202. ISSN: 16849981. DOI: 10.5194/nhess-8-187-2008.

Stoffel, M., Corona, C. (2014). "Dendroecological dating of geomorphic disturbance in trees". *Tree-Ring Research* 70.1, pp. 3–20. ISSN: 15361098. DOI: 10.3959/1536-1098-70.1.3.

Taylor, R., Long, A., Kra, R. (1992). *Radiocarbon after four decades: an interdisciplinary perspective*. Vol. 30. 04, pp. 30–2136. ISBN: 9781475742510. DOI: 10.5860/choice.30-2136.

Techel, F., Pielmeier, C., Darms, G., Teich, M., Margreth, S. (2013). *Schnee und Lawinen in den Schweizer Alpen. Hydrologisches Jahr 2011/2012*. Tech. rep., p. 118.

Tonelli, E., Vitali, A., Piermattei, A., Urbinati, C. (2020). "Are young trees suitable for climate-growth analysis? A trial with Pinus nigra in the central Apennines treeline". *Dendrochronologia* 62.October 2019. ISSN: 16120051. DOI: 10.1016/j.dendro.2020.125720.

Veblen, T. T., Hadley, K. S., Nel, E. M., Kitzberger, T., Reid, M., Villalba, R., Veblen, T. T., Hadley, K. S., Nel, E. M., Kitzberger, T., Reid, M., Villalba, R. (1994). "Disturbance Regime and Disturbance Interactions in a Rocky Mountain Subalpine Forest". *British Ecological Society* 82.1, pp. 125–135.

Wiesinger, T., Aebi, M. (2005). *Schnee und Lawinen in den Schweizer Alpen Winter 2003 /2004*. Tech. rep. Davos: Institut für Schnee- und Lawinen forschung SLF, p. 76.

Wilson, B. F., Archer, R. R. (1977). "Reaction Wood: Induction and Mechanical Action". *Annual Review of Plant Physiology* 28.1, pp. 23–43. ISSN: 0066-4294. DOI: 10.1146/annurev.pp.28.060177.000323.

Wistuba, M., Malik, I. (2012). "Dendrochronological methods for reconstructing mass movements -an example of landslide activity analysis using tree-ring eccentricity". *Geochronometria* 39.3, pp. 180–196. ISSN: 17338387. DOI: 10.2478/s13386-012-0005-5.

Wistuba, M., Malik, I., Gärtner, H., Kojs, P., Owczarek, P. (2013). "Application of eccentric growth of trees as a tool for landslide analyses: The example of Picea abies Karst. in the Carpathian and Sudeten Mountains (Central Europe)". *Catena* 111, pp. 41–55. ISSN: 03418162. DOI: 10.1016/j.catena.2013.06.027.

Wistuba, M., Malik, I., Krapiec, M. (2018). "Can we distinguish between tree-ring eccentricity developed as a result of landsliding and prevailing winds? Consequences for dendrochronological dating". *Geochronometria* 45.1, pp. 223–234. ISSN: 18971695. DOI: 10.1515/geochr-2015-0098.

Zbinden, P. (2010). *2010 Annalen Annales Annali*. Tech. rep., pp. 1–163.

Zweifel, B., Pielmeier, C., Techel, F., Marty, C., Stucki, T. (2021). *Schnee und Lawinen in den Schweizer Alpen. Hydrologisches Jahr 2020/2021.* Tech. rep.

Zweifel, B., Stucki, T., Marty, C., Techel, F., Lucas, C., Hafner, E. (2019). *Schnee und Lawinen in den Schweizer Alpen. Hydrologisches Jahr 2018/2019.* Tech. rep., p. 134.

9 Appendix

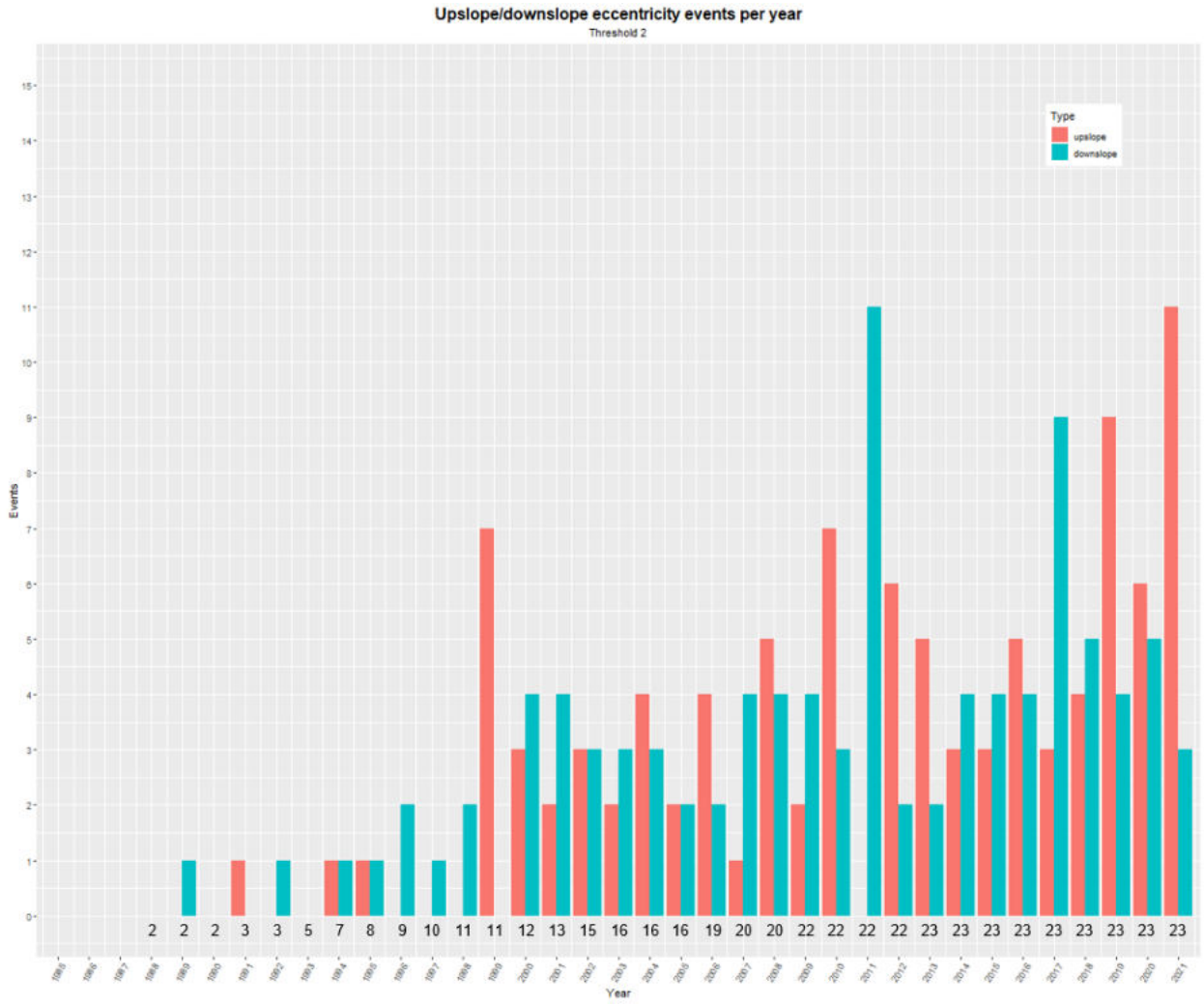

Figure 38: Eccentricity events in sampled birch trees exceeding threshold 2.

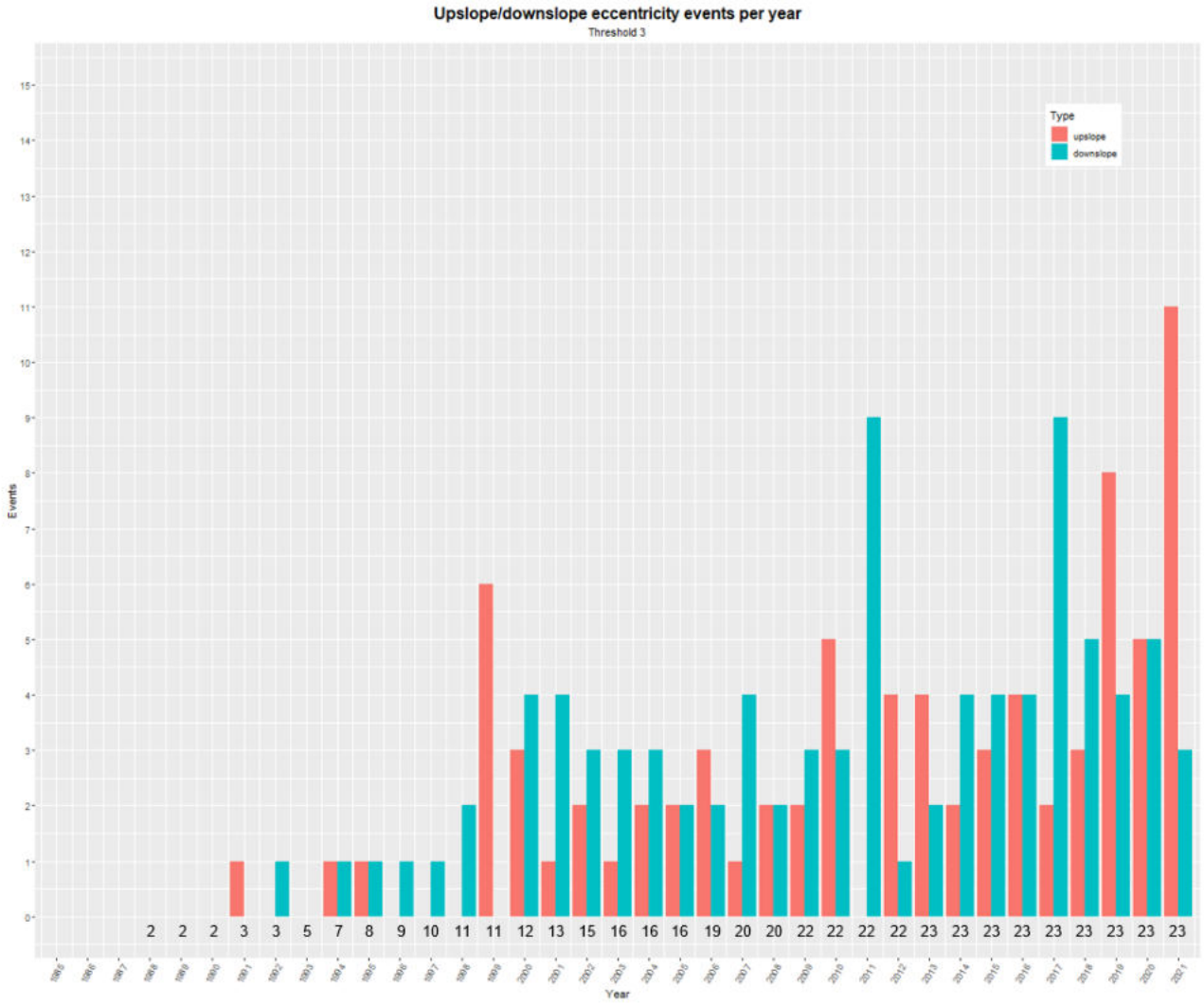

Figure 39: Eccentricity events in sampled birch trees exceeding threshold 3.

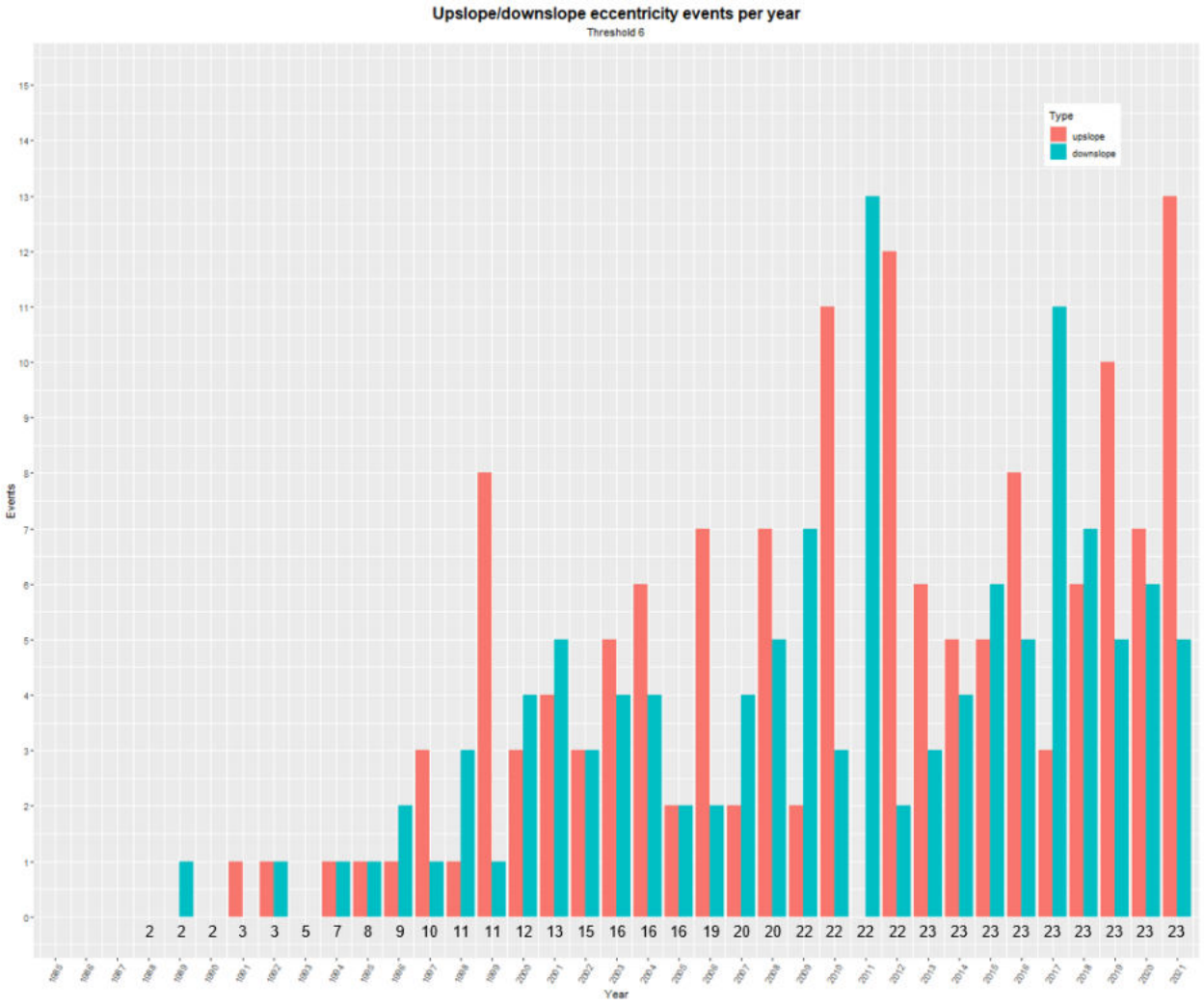

Figure 40: Eccentricity events in sampled birch trees exceeding threshold 6.

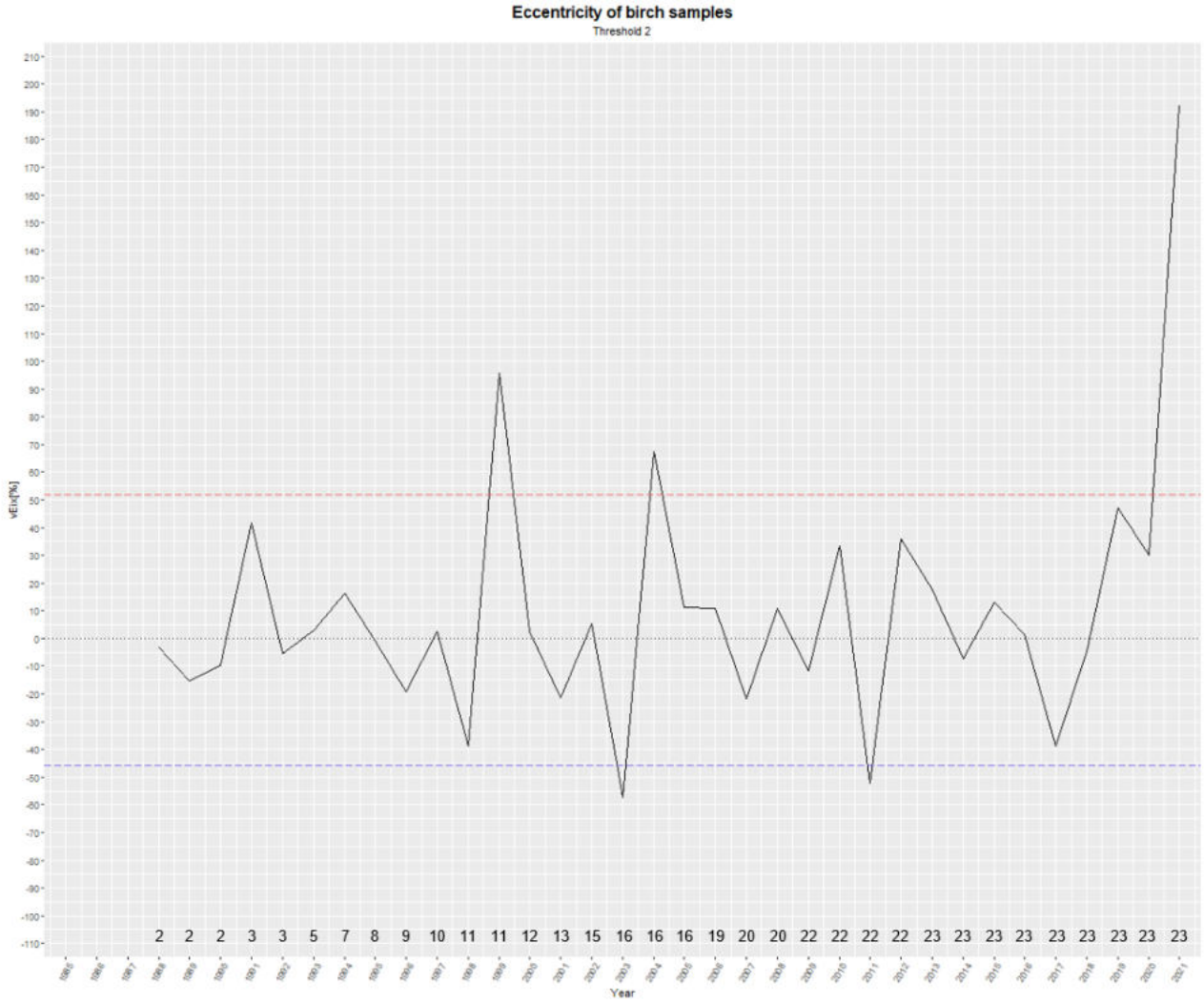

Figure 41: Eccentricity events of birch trees being marked by horizontal lines. Here, threshold 2 is used.

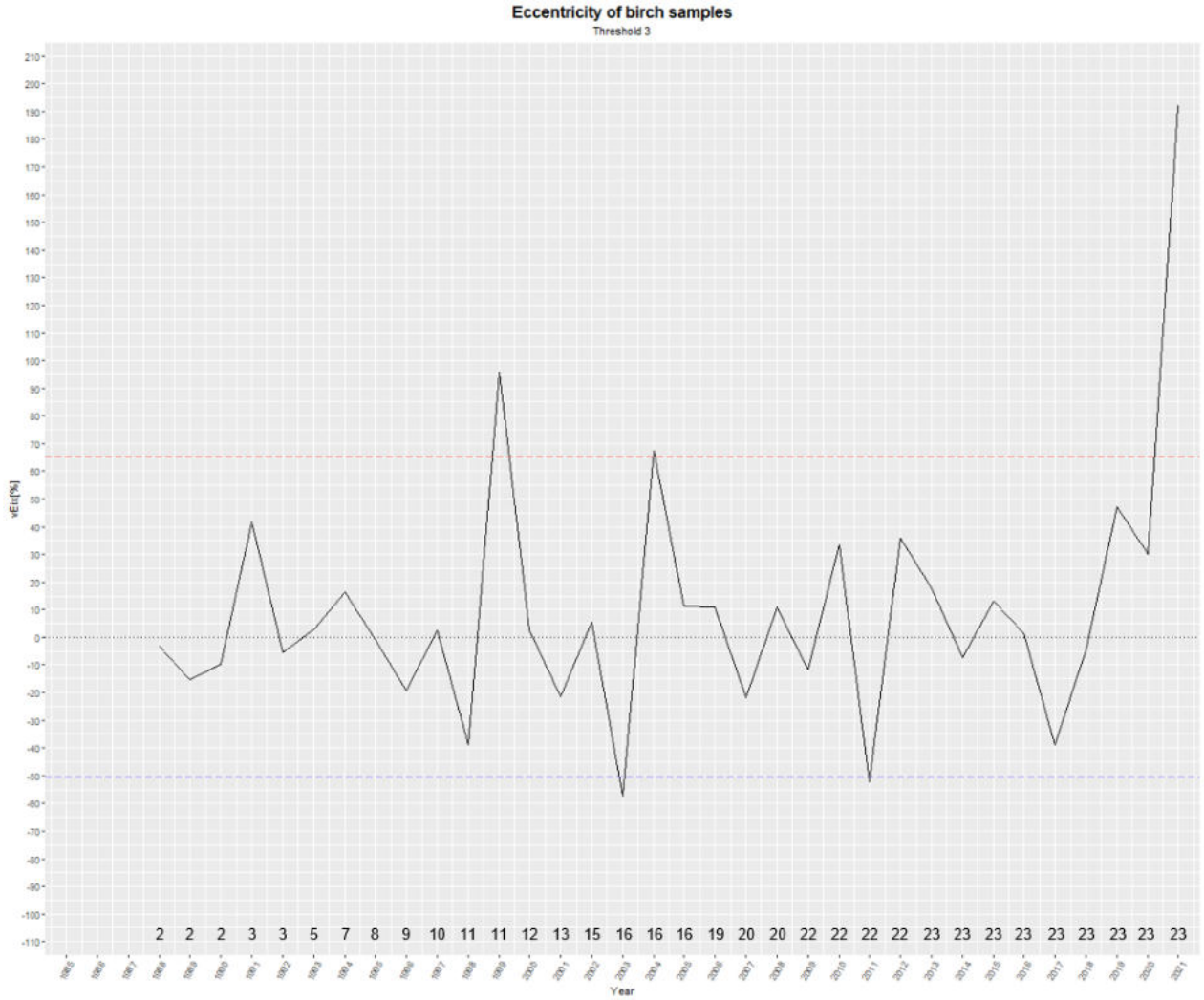

Figure 42: Eccentricity events of birch trees being marked by horizontal lines. Here, threshold 3 is used.

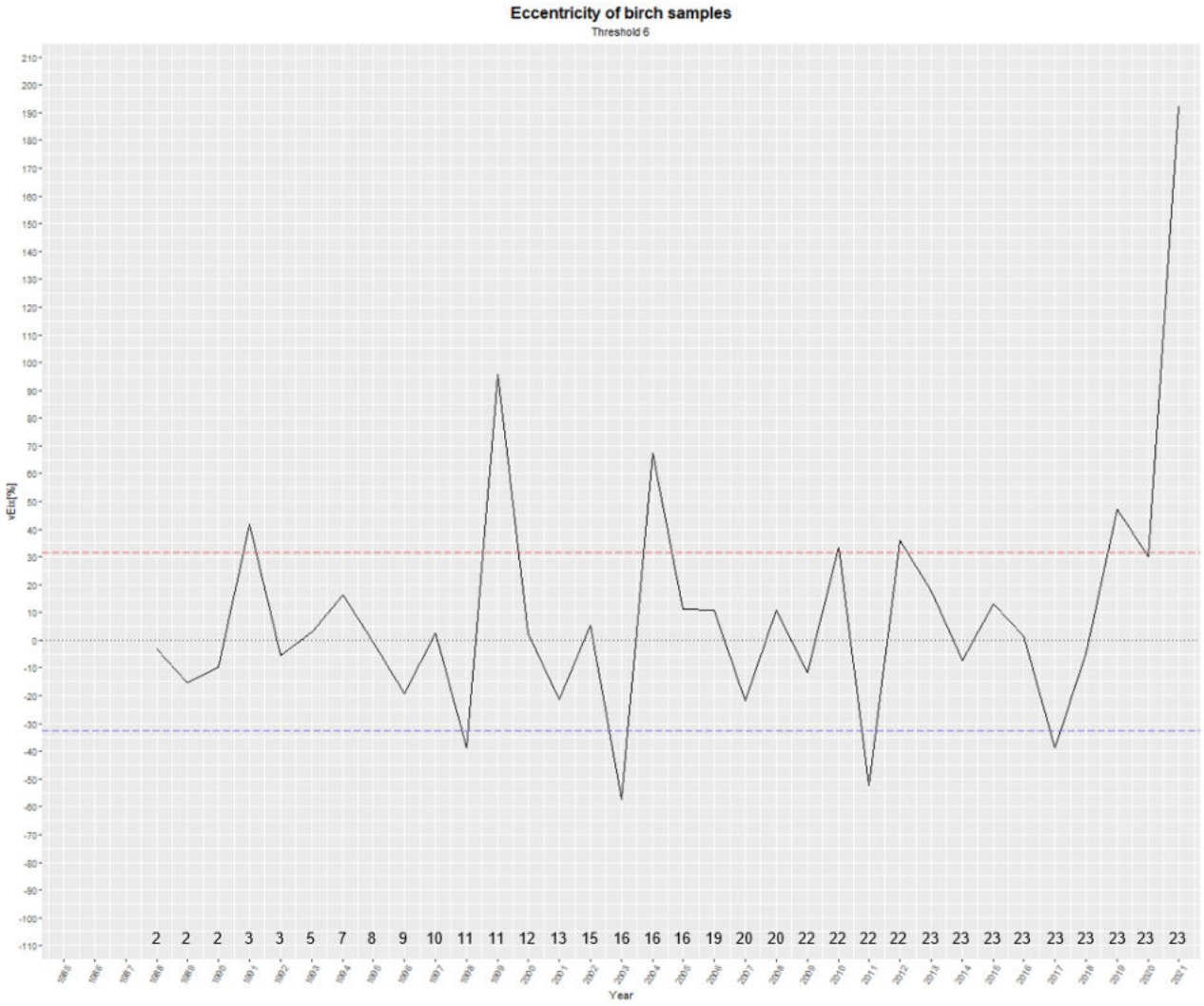

Figure 43: Eccentricity events of birch trees being marked by horizontal lines. Here, threshold 6 is used.

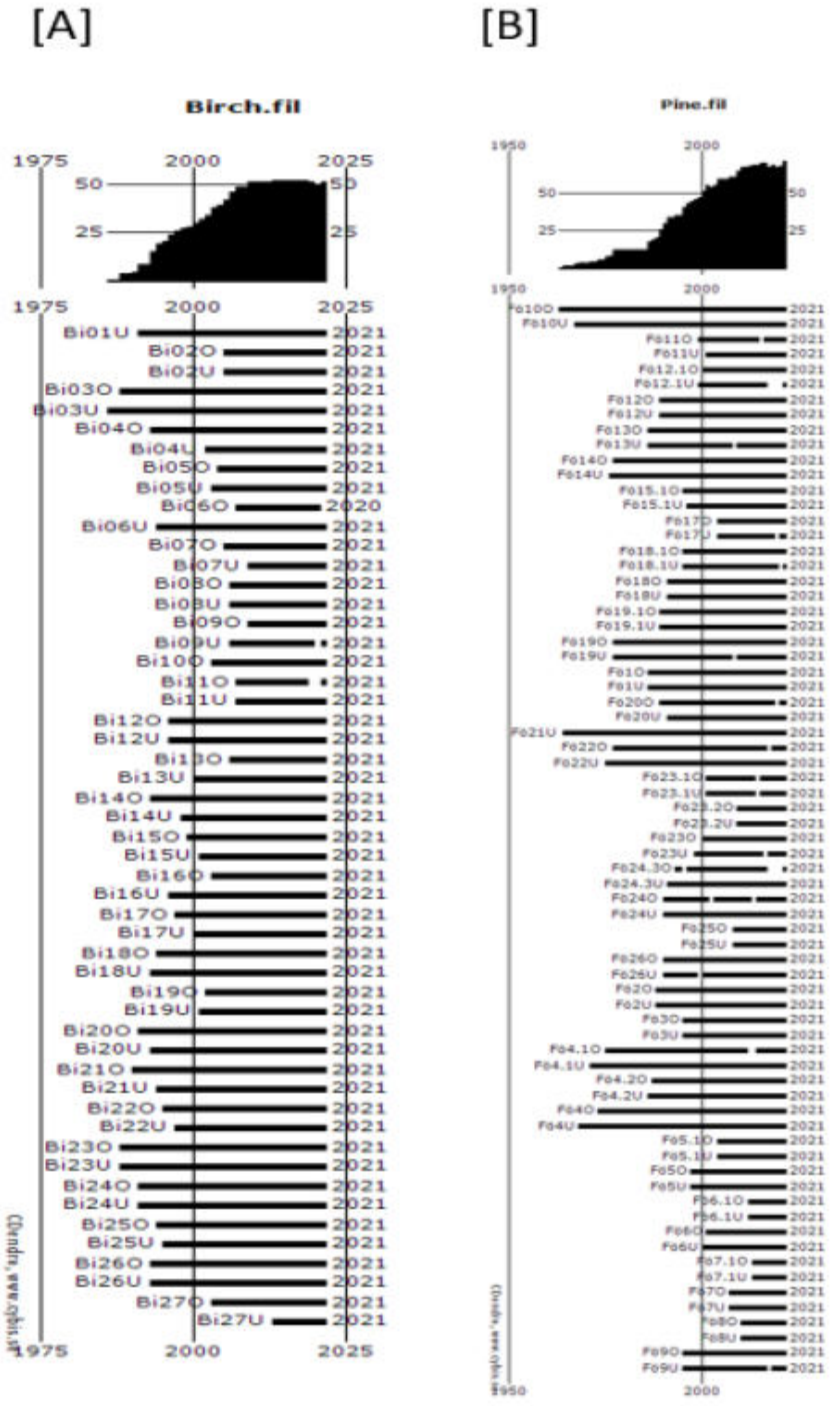

Figure 44: Diagrams of the sampled trees in [A] the birch and in [B] the mountain pine. The ages of the samples are given on the x-axis, each horizontal bar representing one sample. On top, the plot of the sample depth is shown. The plot was arranged with CDendro.

Figure 45: Many rocks and boulders at the study site indicate a high rockfall activity.

Figure 46: Pushed over and strongly bent trees on the eastern side of the study site.

Personal declaration: I hereby declare that the submitted Thesis is the result of my own, independent work. All external sources are explicitly acknowledged in the Thesis.

Andermatt, 31.01.2022

Location, Date

Philipp Rüegg